Nuclear Cardiology
Background of the basics

David Stultz, MD

December 8, 2005

Cardiology Fellow, PGY-6

Radiation is like Football

Think of the Football as the radiation (X-ray, Gamma ray, positron, etc)…

Think of the Quarterback as the source of the radiation…

Technitium-99m

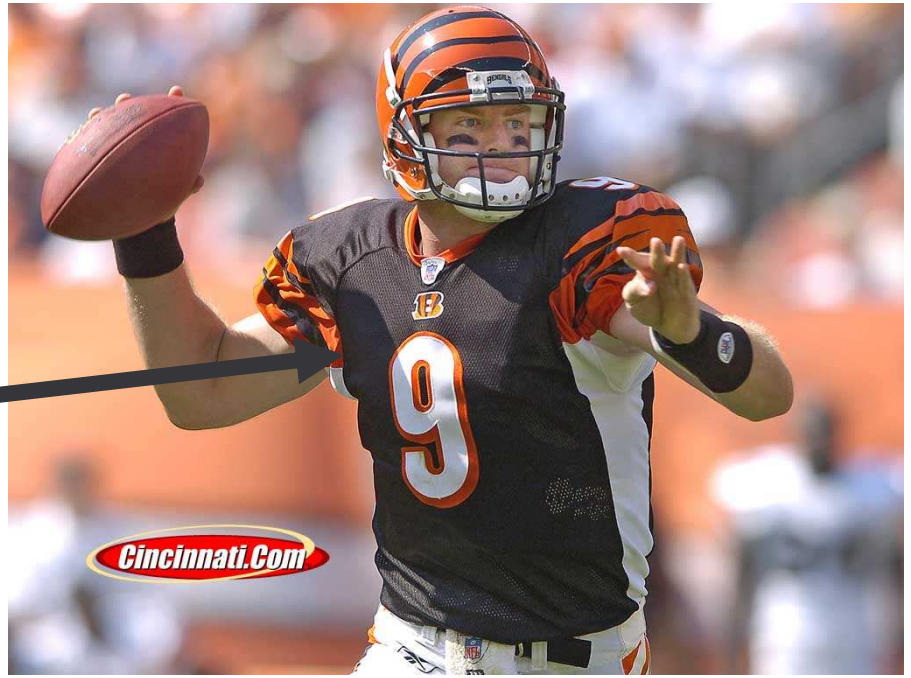

The Quarterback passes the ball to the Receiver

NaI Crystal

Radiation Hits its Target!

Think of the receiver as a target (target organ, imaging crystal, etc.). When the receiver catches the ball, it was an effective pass.

Sometimes the Receiver Misses

Difference between exposure (pass attempts) and absorption (completions)

Sometimes the ball is run

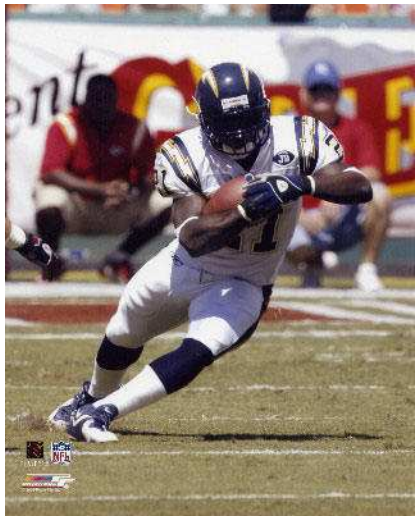

But sometimes he can't run in a straight line

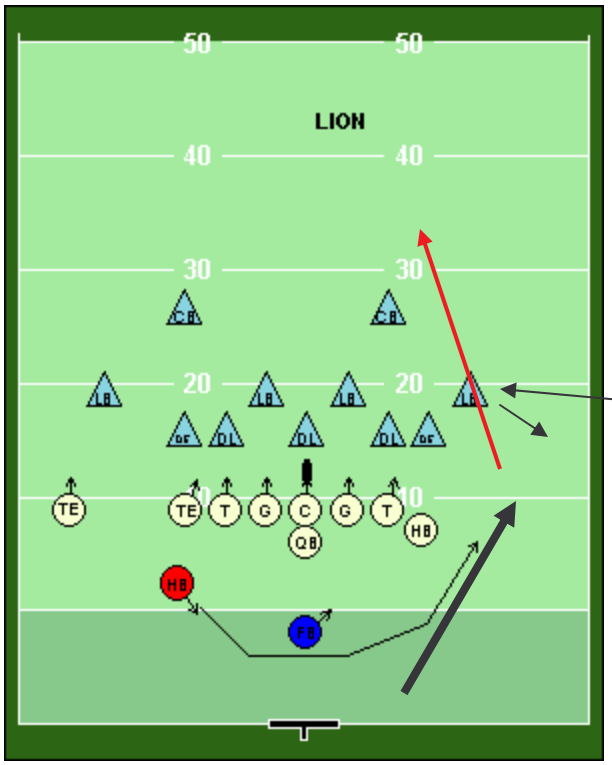

So the Football ends up going this way

But this guy may move to block the way

Scatter

RB wants to go this direction

Types of Radionuclides

TABLE 2.8 *Characteristics of Radionuclides Used in Gamma Ray Imaging*

Nuclide	*Half-life*	*Photon Energies (keV)*	*Γ^*_{20} (R/(hr-mc)@1 cm)*	*HVL (mm Pb)*	*HVL (cm tissue)*
F-18	110 min	511	5.7	3.9	7.0
Co-57	271 days	123	0.56	0.2	4.0
Tc-99m	6 hr	140	0.59	0.3	4.5
Cs-137	30 yr	662	3.26	6.5	7.5
Tl-201	73.1 hr	68-80, 135, 167	0.45	0.2	3.5

*For photons greater than 20 keV.
Γ, specific gamma constant; HVL, half value layer.

TABLE 2.12 *Accelerator-Produced Radionuclides*

Radionuclide	*Half-life*	*Reaction*
O-15	2 min	N-14 (d,n) O-15
		N-15 (p,n) O-15
F-18	110 min	O-18 (p,n) F-18
Co-57	271 days	Fe-56 (d,n) Co-57
Ga-67	78.2 hr	Zn-68 (p,2n) Ga-67
I-123	13.2 hr	Sb-121 (α,2n) I-123
Tl-201	73 hr	Tl-203 (p,3n) Pb-201,
		Pb-201 → Tl-201

Radiation Units

A. UNITS OF RADIOACTIVITY	
Curie (Ci)	= 37×10^9 dps
Millicurie (mCi)	= 37×10^6 dps
Becquerel (Bq)	= 1 dps
Megabecquerel (MBq)	= 10^6 *dps*
1 mCi	= 37 MBq

Dps = Disintigrations per second

Units of Radioactivity

B. UNITS OF RADIOACTIVITY EXPOSURE

Roentgen (R): A measure of the ionization of molecules caused by x-rays or gamma rays

Rad (radiation absorbed dose): Measure of absorbed dose of any type of radiation

Gray (Gy): SI unit of absorbed dose

1Gy ≈ 100 rads

Rem (roentgen equivalent man): Unit of absorbed dose in human tissue equivalent to its biologic damage

Sievert (Sv): SI unit of equivalent dose

1 Sv = 100 rem

1 gray = 100 rad, since

1 joule = 10^7 erg

1 kg = 10^3 gm

1 gray = 1 joule/kg = 10^7 erg/10^3 gm

= 10^4 erg/gm = 100 rad

TABLE 2.15 *Quantities and Units in Dosimetry*

Quantity	*Traditional Unit*	*International Standard Unit*
Exposure	Roentgen	Coulombs/kilogram
Absorbed dose	Rad	Gray
Dose equivalent	Rem	Sievert
Equivalent dose	Rem	Sievert
Effective dose equivalent	Rem	Sievert
Effective dose	Rem	Sievert
Activity	Curie	Becquerel

TABLE 2.23 *A Range of Doses*

Radiation Exposure	
PA chest film-entrance skin dose	0.3 mSv
Average USA background	3 mSv
Declared pregnancy dose limit	5 mSv
KUB-entrance skin dose	5.5 mSv
Tc^{99m} MIBI effective dose (30 mCi)	8.8 mSv
Tl^{201} effective dose (5 mCi)	41 mSv
CT of the body	20–40 mSv
Occupational TEDE*	50 mSv/year
Occupational eye dose limit	0.15 Sv
Occupational extremity dose limit	0.5 Sv
Erythema	2 Sv
LD_{50} man	4.5 Sv
Tumor treatment dose	60 Sv

*Total effective dose equivalent.

TABLE 2.22 *Annual Regulatory Dose Limits in USA*

Radiation worker	50 mSv total effective dose equivalent*
	150 mSv lens of eye
	500 mSv skin
	500 mSv any organ or extremities
Member of the public	1 mSv total effective dose equivalent*
	0.02 mSv in any one hour
Fetal dose of declared pregnant worker	5 mSv over term of pregnancy
	<0.5 mSv /month recommended

*Sum of the external and internal dose equivalents.

Acquisition

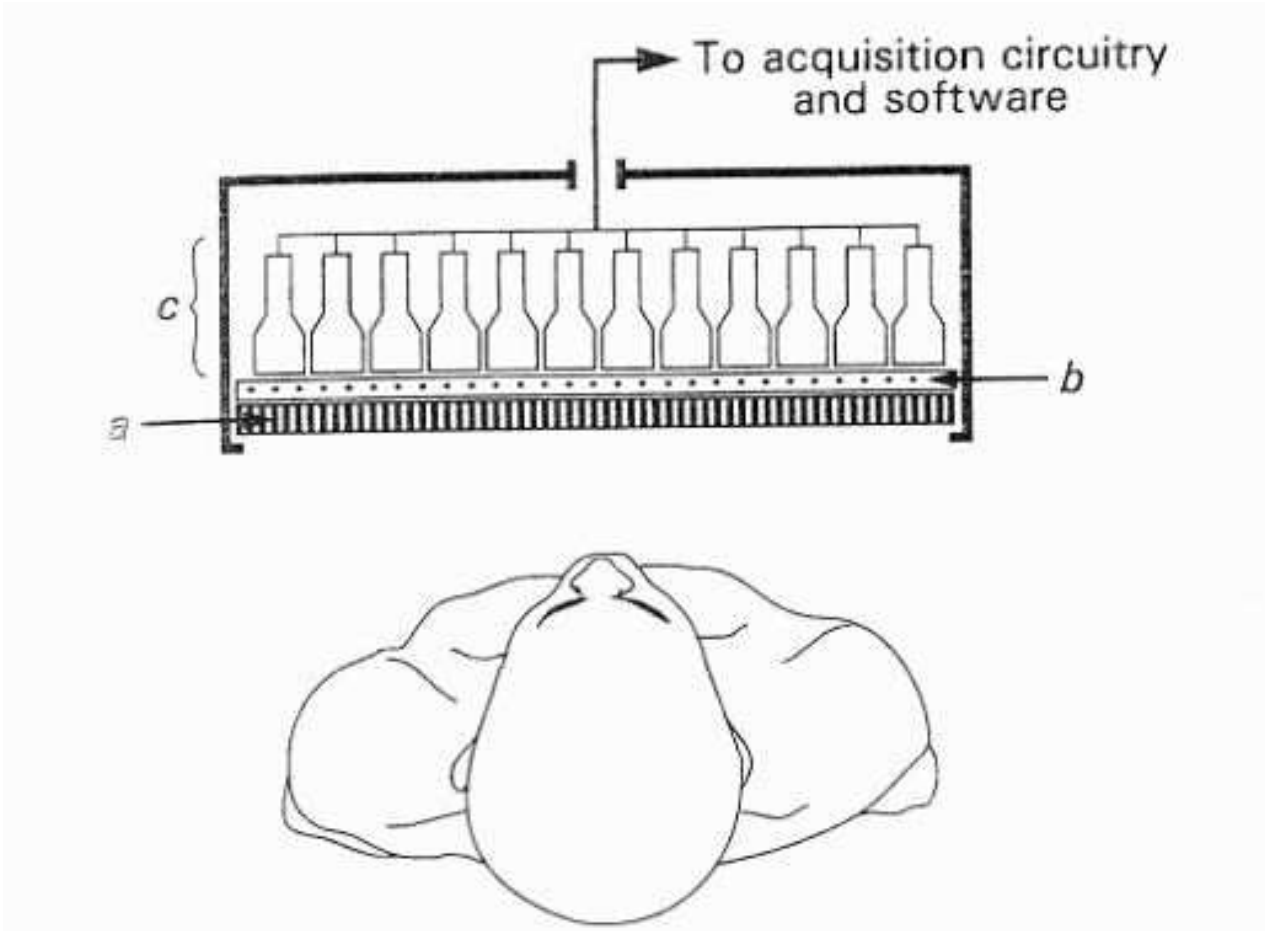

FIGURE 3.1 Cross-sectional view of the three basic components of a gamma camera head. (*a*) collimator; (*b*) scintillation crystal; and (*c*) photomultiplier array.

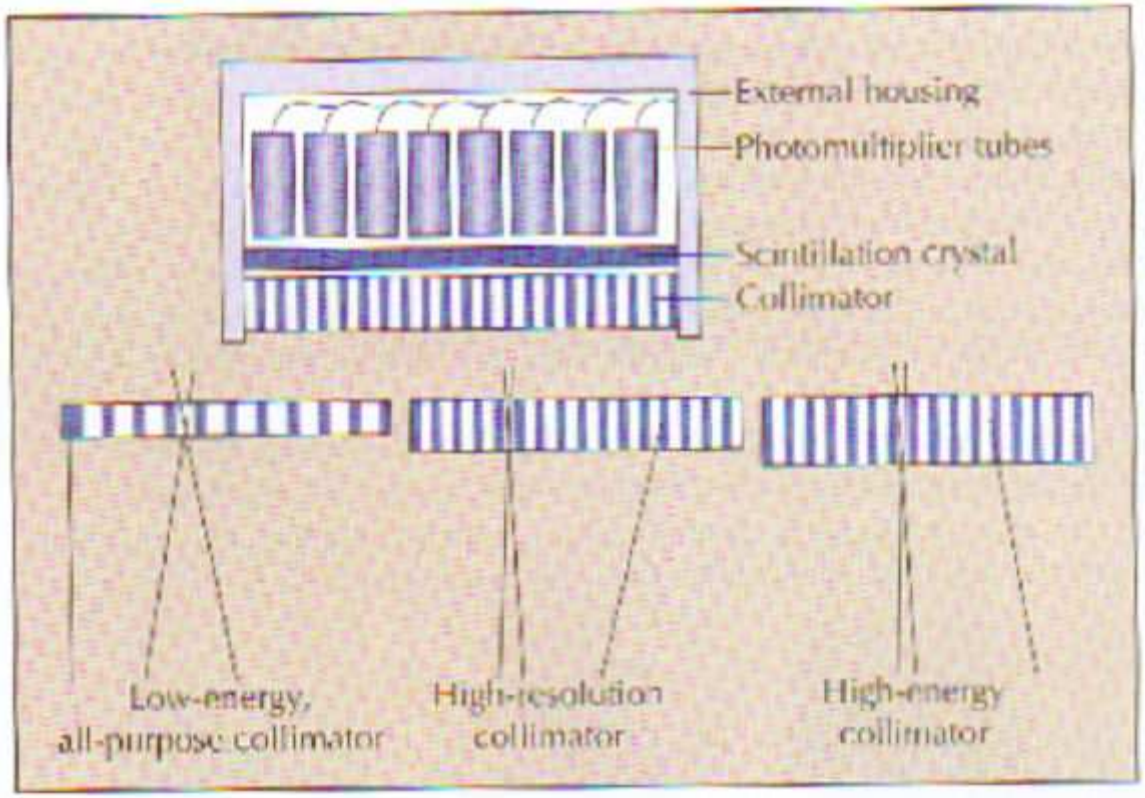

FIGURE 1-17. Structure of a gamma camera. The components of a gamma camera include the 1) scintillation detector, 2) photomultiplier tubes, 3) collimator, and 4) computer and electronics.

Scintillation detector. The scintillation detector, made up of sodium iodide or bismuth germanate (BGO), absorbs gamma rays and converts them into visible light. A gamma ray travels through the

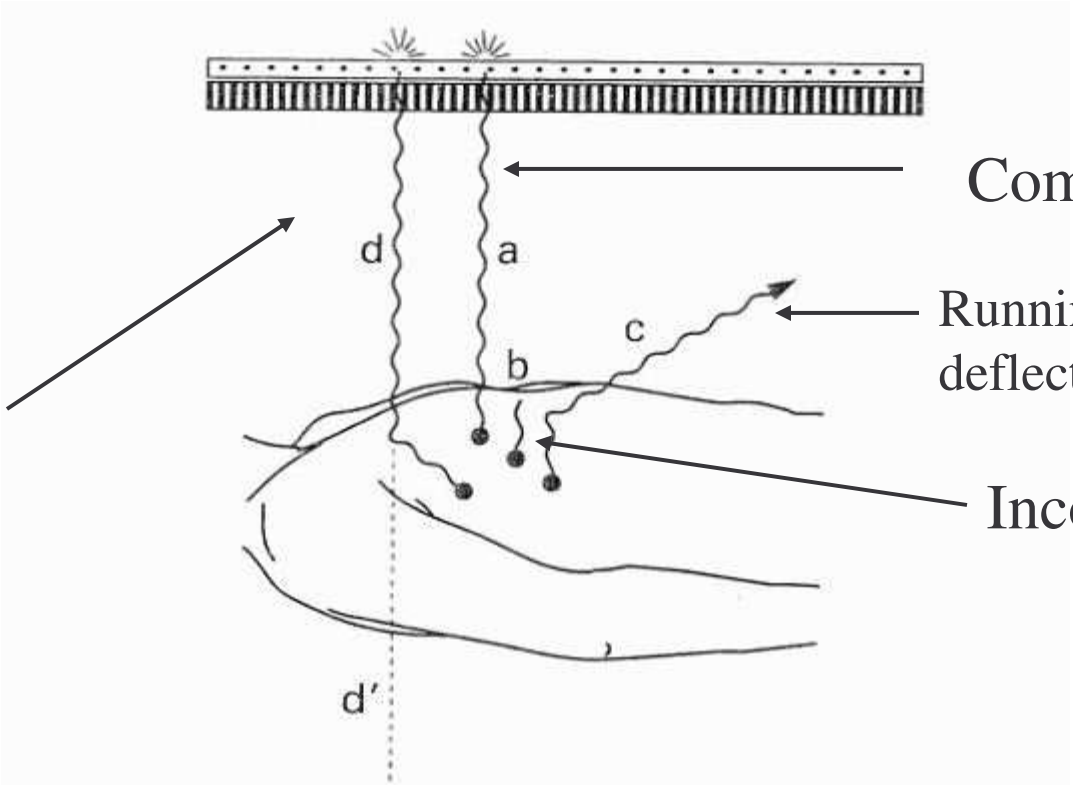

Completed pass!

Running back
deflected by defender!

Interception?

Incomplete pass!

FIGURE 3.2 Possible fates of photons emanating from an organ perfused with a labeled compound: (*a*) an image-forming unscattered photon reaching the scintillation crystal; (*b*) a photon that has suffered complete (photoelectric) absorption before leaving the body; (*c*) a photon initially headed to the camera with an image-forming trajectory but that is then scattered away from the camera; (*d*) a photon that is scattered toward the detector and distorts the image by masquerading as having originated along trajectory *d′*.

Scatter

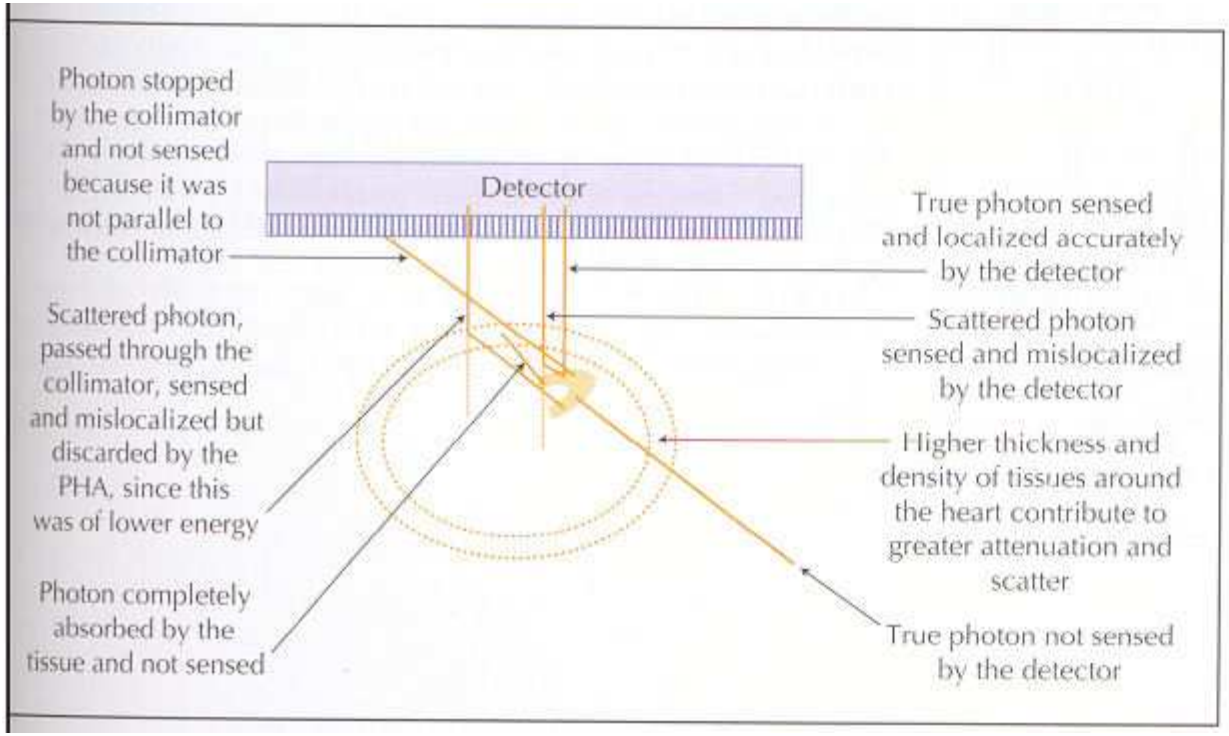

FIGURE 1-20. Detection of gamma rays by the detector. A gamma ray originating from the heart can have any of the following fates:

The gamma ray can pass through the overlying tissues and hit the collimator on one of its holes parallel to the direction of the holes. When the gamma ray falls on the scintillation detector and gets converted into a speck of light, it will be detected by a photomultiplier tube and registered as a photon by the electronics of the system.

The gamma ray can pass through the body and exit in a space that is not facing the gamma camera. This is a wasted photon. Use of multiple detectors maximizes photon detection.

Continued on next page

Spatial Resolution

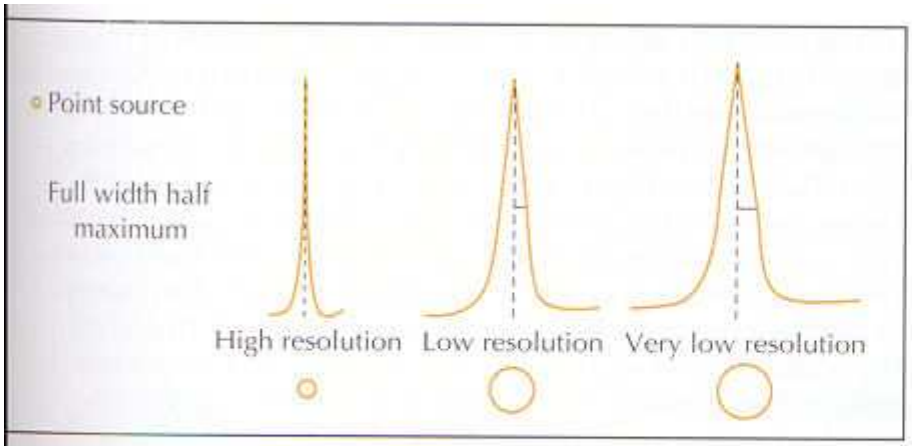

FIGURE 1-18. Spatial resolution and point spread function. Three parameters contribute to the technical adequacy of the radionuclide images: 1) spatial resolution, 2) noise, and 3) contrast.

Spatial resolution is instrument- or hardware-dependent. The limitations of spatial resolution make a point source appear as a dot, rather than a point, during imaging with a gamma camera. The intrinsic resolution of an imaging system is described by point spread function or by obtaining the full width at half-maximum. With improvements in detector and collimator design and electronics, the intrinsic resolution of the gamma cameras has improved significantly over the last decade. Currently, this resolution is on the order of 3 to 4 mm.

Noise is irrelevant information or a disturbance of the useful data in the image. Noise can be filtered out by applying appropriate filters.

Contrast is a measure of the intensity or counts in a target organ compared with the intensity in the background region, and is often measured as a difference in the counts between the target organ and the background divided by the background counts. The higher the contrast, the more visible the organ of interest.

Partial Volume Effect

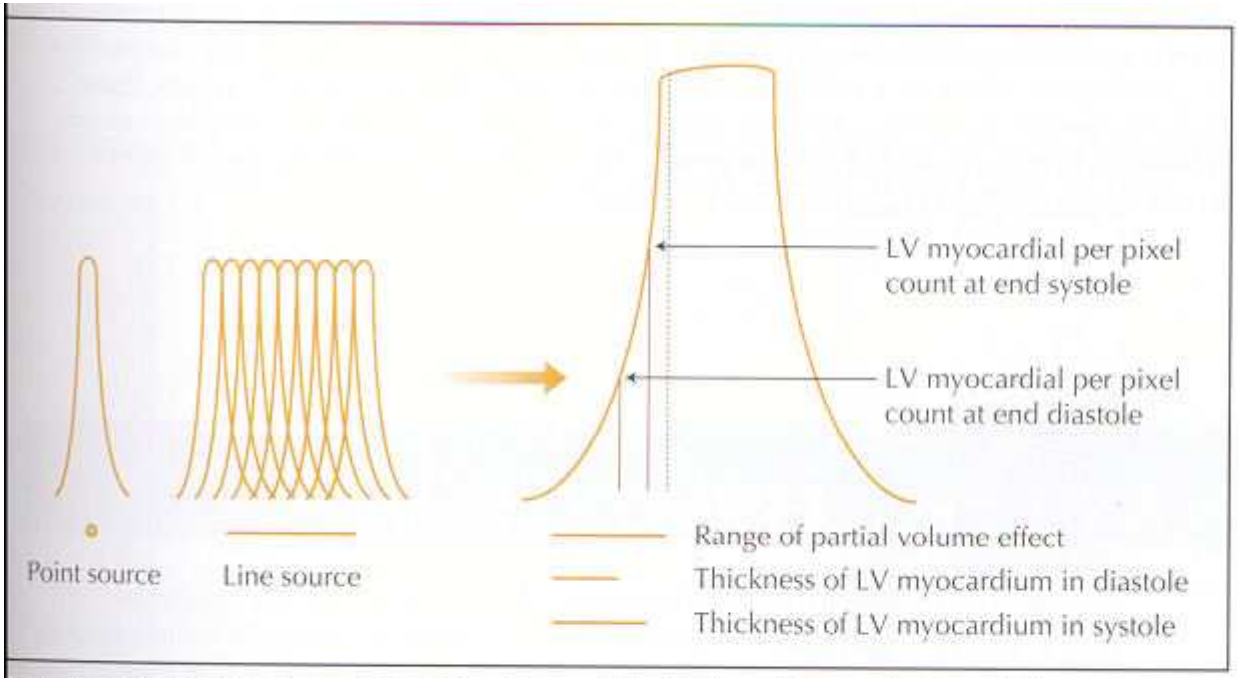

FIGURE 1-19. Partial volume effect. The inherent limitation of the resolution of the nuclear imaging systems makes the image of a point source appears as a dot of variable size, depending on the resolution of the system. Each point appears as a gaussian curve. An object being imaged (which can be considered to be made up of multiple, successive points) appears as overlapping dots. As a result of this overlap, the object appears brighter at the center than at the periphery, even when the imaged object has uniform distribution of the radiotracer. An important resultant of this phenomenon occurs during gated SPECT imaging. The left ventricular (LV) myocardial thickness varies during the cardiac cycle. The myocardium is thicker during systole than during diastole. Consequently, the myocardium appears brighter during systole than during diastole. The increase in myocardial brightness during systole compared with the myocardial brightness in diastole is an artifact of partial volume effect. However, this technique is used quite successfully in nuclear imaging to assess regional myocardial thickening during the cardiac cycle.

TABLE 3.1 *Attenuation Values in Water (~Tissue), Lead (Collimator), and NaI (Crystal) for Isotopes Commonly Used in Nuclear Cardiology*

Nuclide	*Energy (keV)*	*μ (water) (1/cm)*	*μ (lead) (1/cm)*	*μ (NaI) (1/cm)*	*HVT (water) (cm)*	*HVT (lead) (cm)*	*HVT (NaI) (cm)*
Tl-201	71	0.18	20.38	14.44	3.85	0.034	0.048
Tc-99m	140	0.15	24.75	2.62	4.50	0.028	0.265
Fl-18 (β+)	511	0.10	1.69	0.34	7.10	0.410	2.050

μ, coefficient of linear attenuation; HVT, half-value thickness.

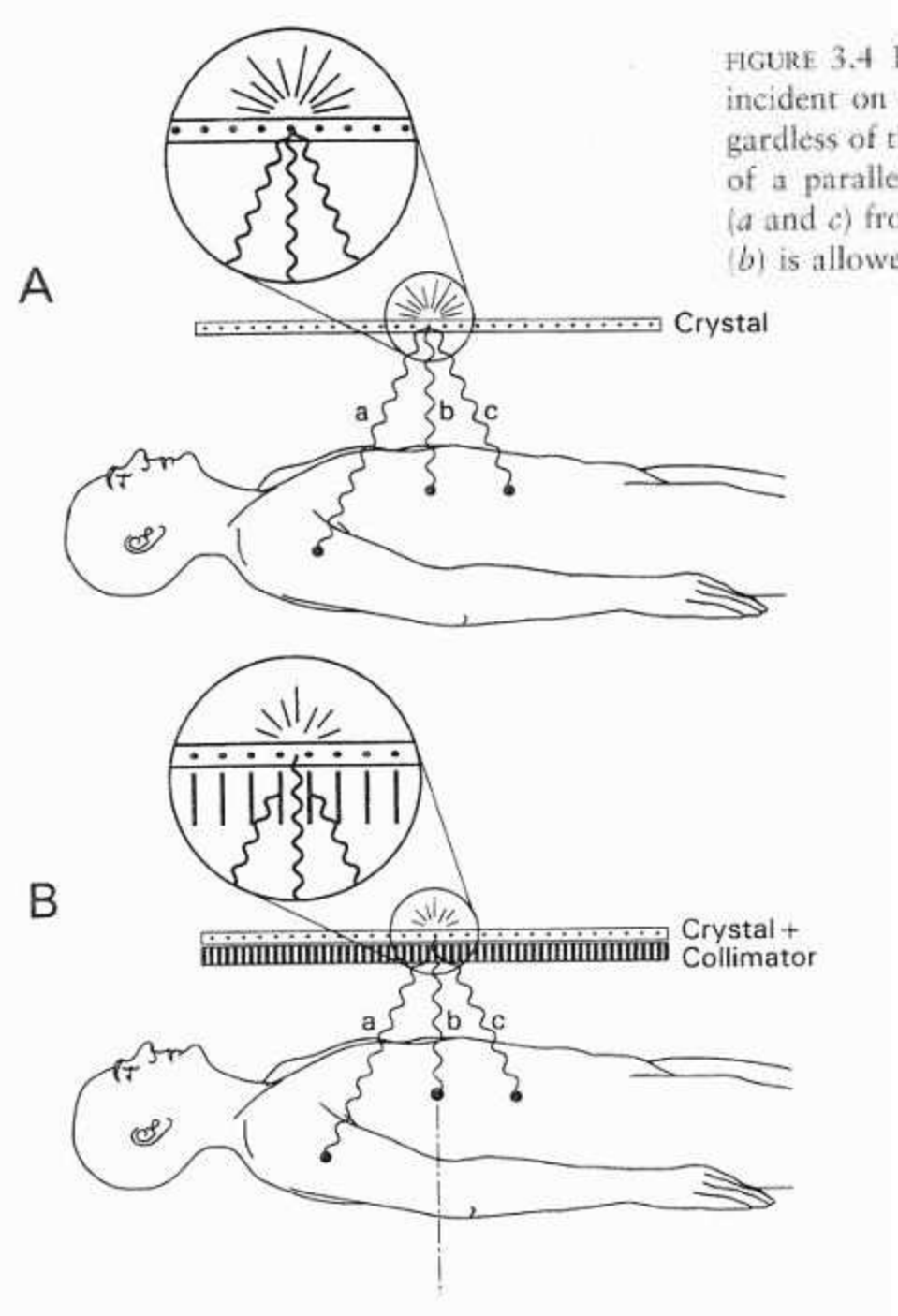

FIGURE 3.4 Effect of a collimator. (*A*) Without collimator, photons incident on a given point in the crystal will cause scintillations regardless of their trajectory and no image is formed. (*B*) The presence of a parallel-hole collimator excludes non-image-forming photons (*a* and *c*) from the imaging process while the image-forming photon (*b*) is allowed to reach the crystal (inset).

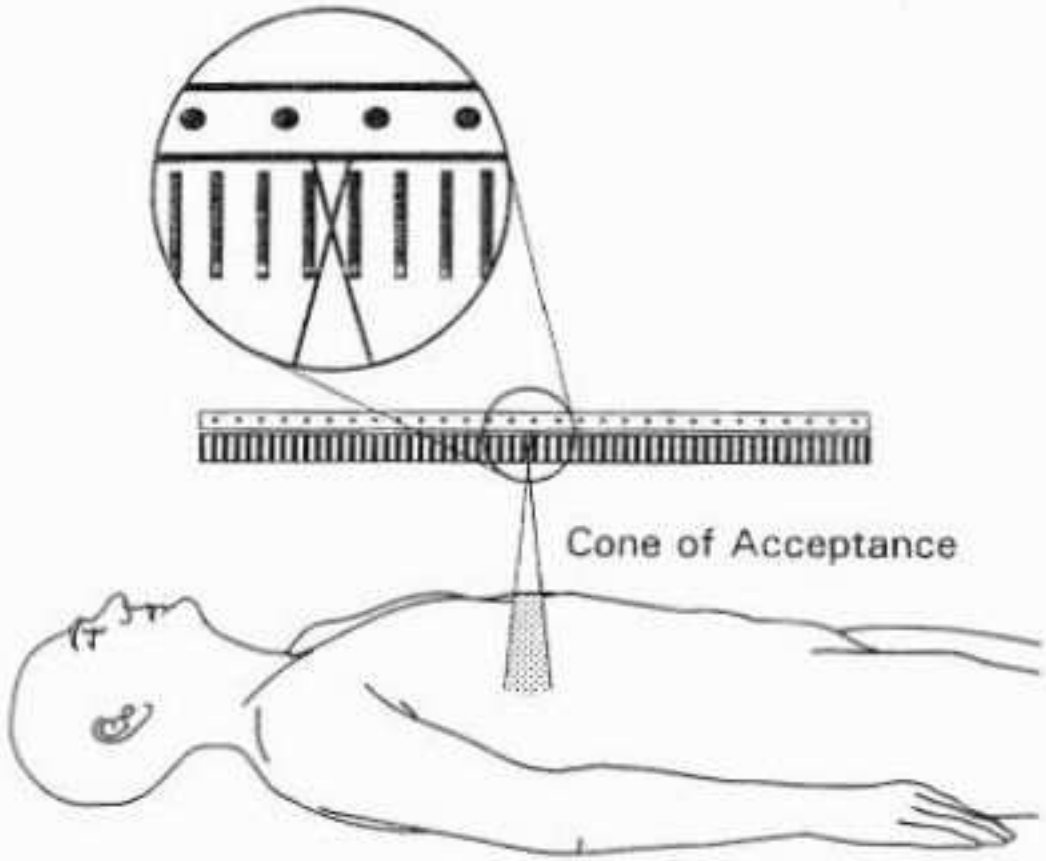

FIGURE 3.5 A detailed view of a collimator hole showing the conical shape of the photon-accepting region. Any photon with all its trajectory within that cone will be considered image-forming and will reach the crystal. The width of the cone, therefore, represents the inherent uncertainty in the direction of a photon passing through a collimator hole. The larger the distance from the collimator, the wider is the cone, the more uncertain is the direction. The cone shown is exaggerated in size for illustrative purposes.

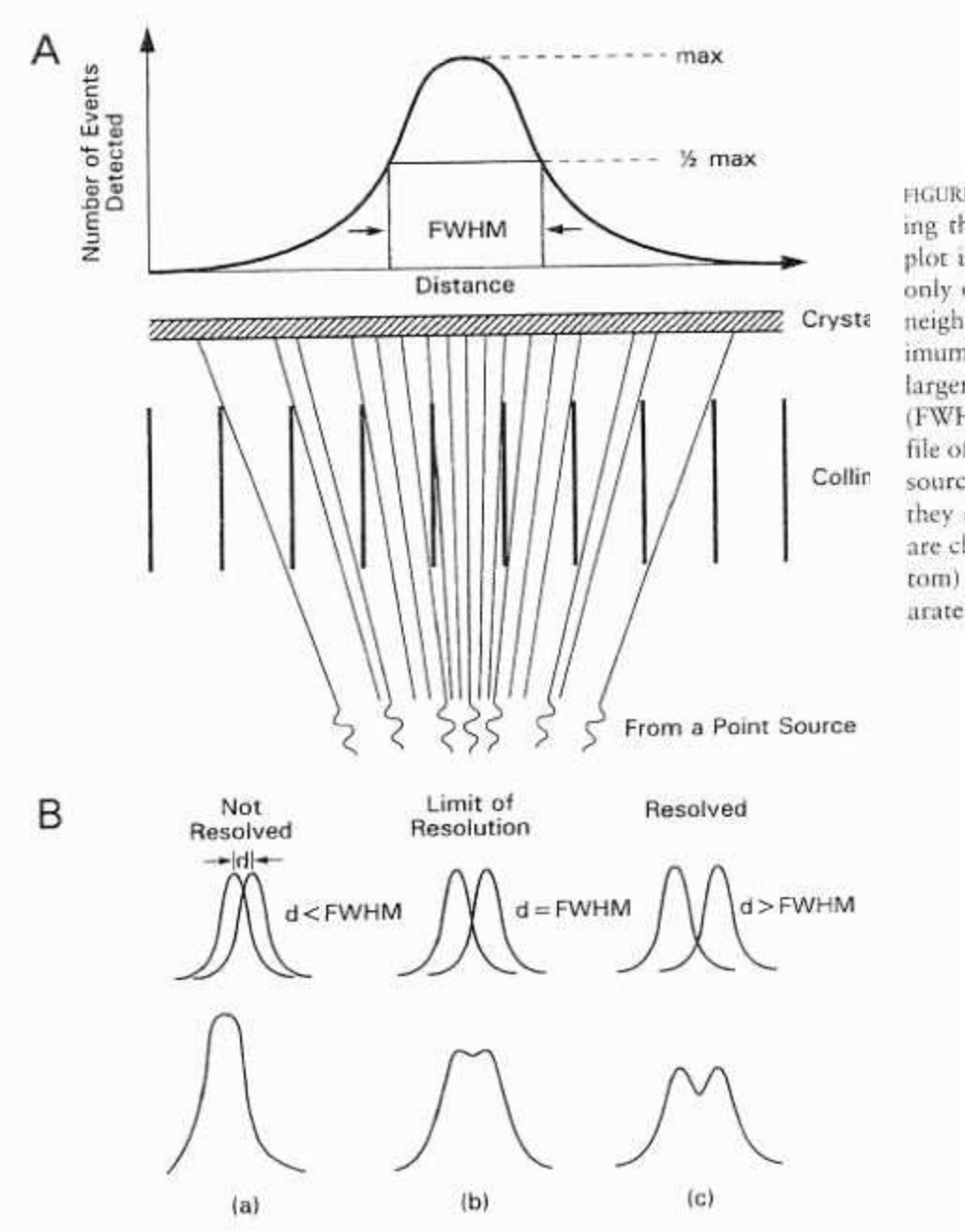

FIGURE 3.6 (*A*) A plot of count rate vs. position obtained by exposing the camera head to a point source. At any given distance this plot is Gaussian shaped. Ideally, a point source should be 'seen' by only one collimator hole. Instead overlap in the acceptance cones of neighboring holes causes some spillover of counts, affecting the maximum achievable resolution. The distance encompassing count rates larger than half the maximum, or full width at half maximum (FWHM), is a measure of the camera resolution. (*B*) The count profile of two point sources at three different separations. The two point sources are considered detectable as two separate sources only when they are separated by at least one FWHM (*b* and *c*). If the sources are closer than a FWHM, their combined profiles (curves at the bottom) become difficult to distinguish as having arisen from two separate sources.

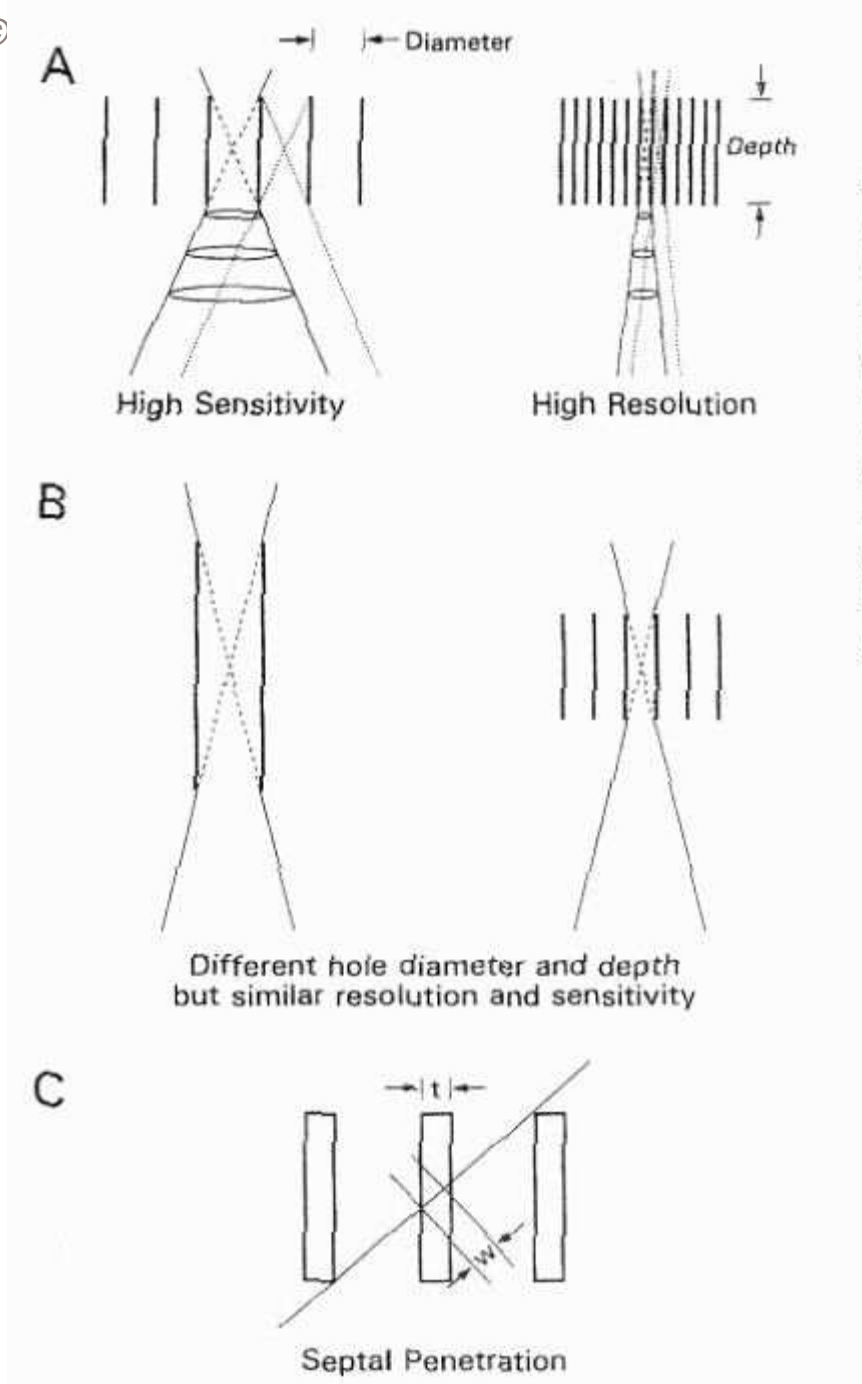

FIGURE 3.7 Effect of collimator hole diameter and depth: (*A*) Two collimators with same depth but different diameter. The wider holes on the left-hand side provide higher sensitivity as they accept a wider range of trajectory angles but at the cost of poorer resolution. The collimator with narrower holes, to the right, has cones of acceptance that overlap less, has less uncertainty about the point of origination of the photons, and therefore has better resolution than the one on the left. However, the increased resolution comes at the cost of reduced sensitivity. (*B*) These two collimators have similar sensitivity and resolution by combining different diameter and depths. (*C*) A third parameter of collimator design is the septal thickness, t. The distance *w* indicates a possible path for septal penetration by th

Photomultiplier

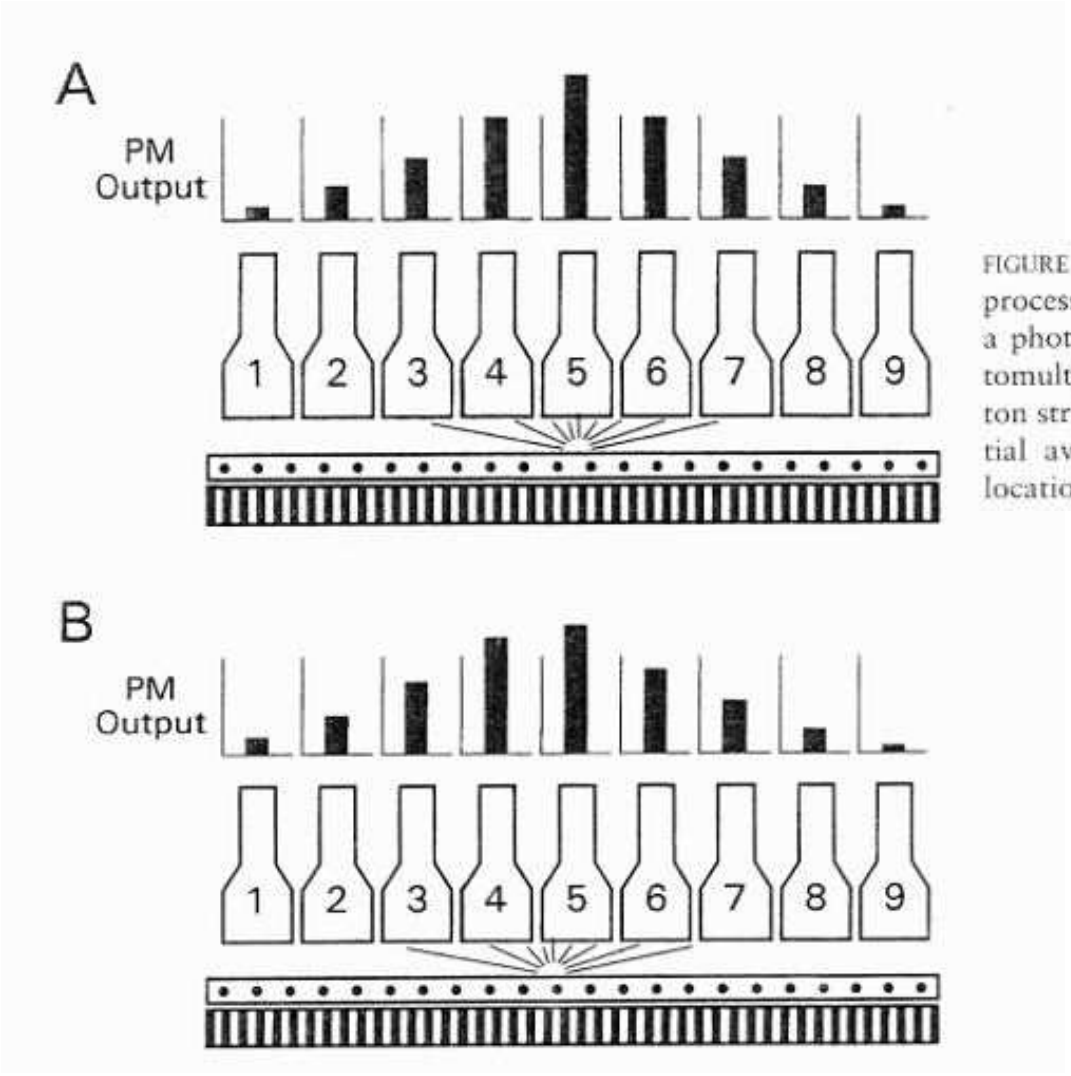

FIGURE 3.10 One-dimensional illustration of the event localization process. (*A*) Symmetric response of neighboring photomultipliers as a photon strikes the crystal at a point exactly centered under photomultiplier #5. (*B*) Asymmetric photomultiplier response as the photon strikes slightly to the left of photomultiplier #5. A weighted, spatial average of the photomultiplier outputs determines the exact location of the event in either case.

Energy Detection

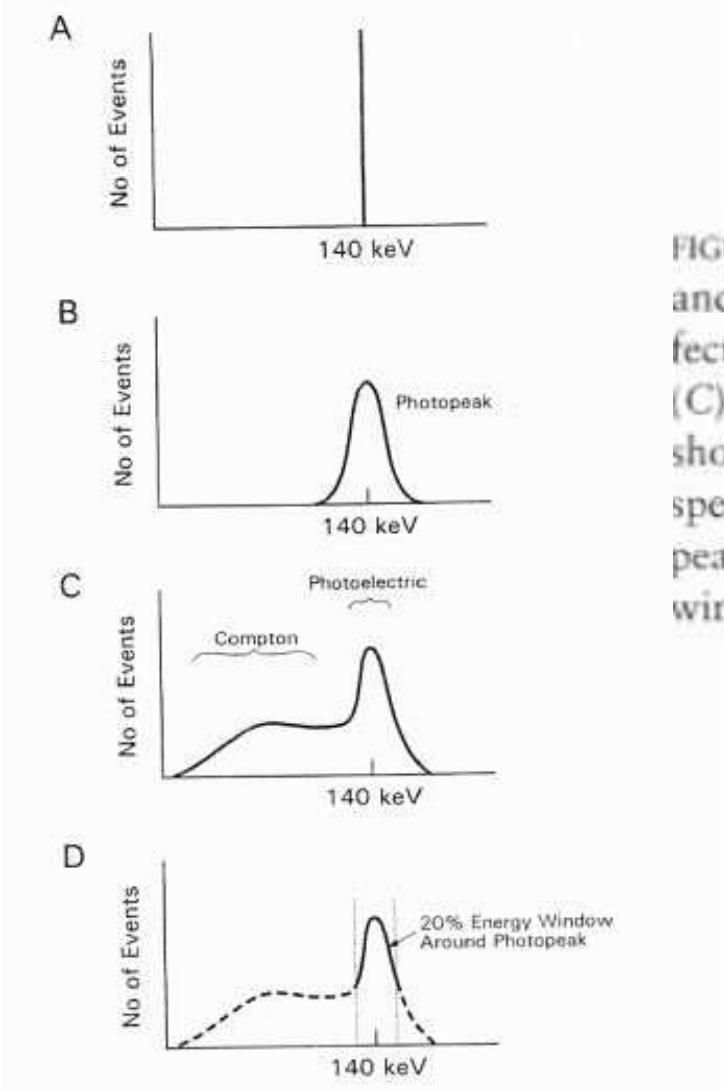

FIGURE 3.11 (*A*) Ideal spectrum of a Tc-99m emitter (no scattering and perfect energy resolution). (*B*) Same as *A* but showing the effects of the finite energy resolution of the crystal/PM tube array. (*C*) Approximate appearance of an actual spectrum from a patient, showing Gaussian smear due to instrumental uncertainties plus the spectral component of Compton scattering to the left of the photopeak. (*D*) Part of the spectrum selected electronically by an energy window with a width of approximately 20% of the photopeak.

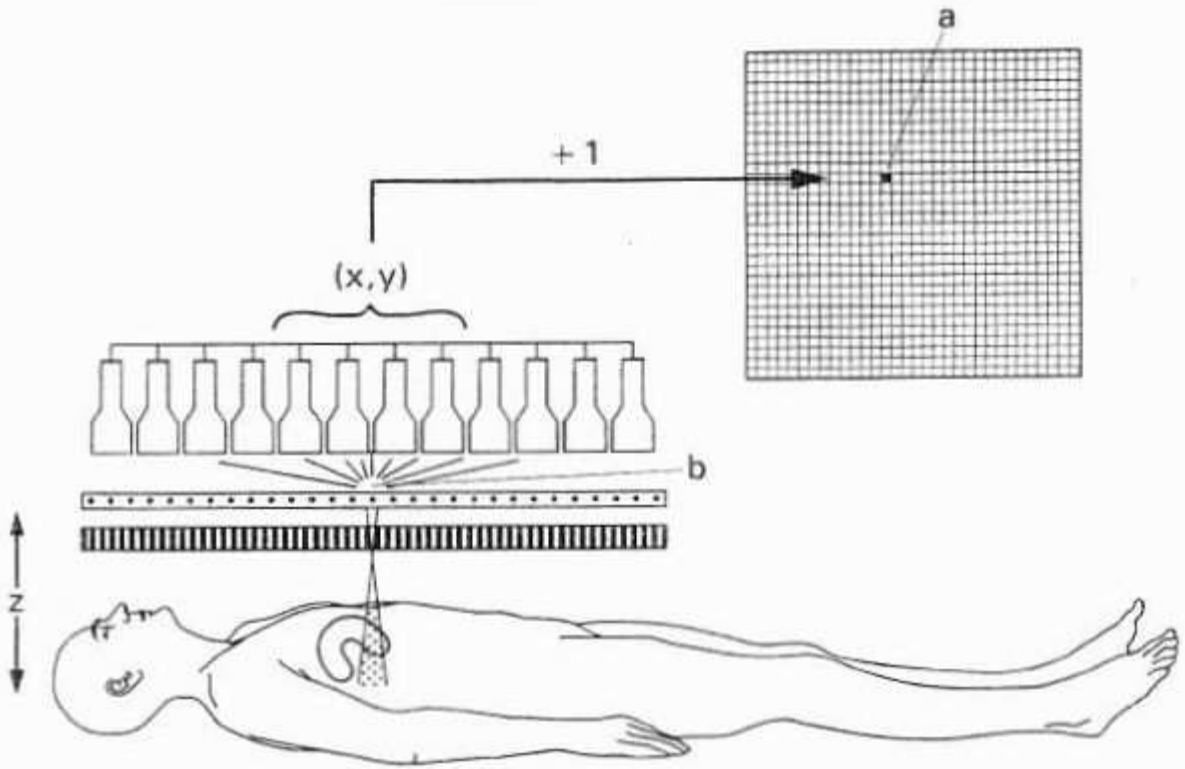

FIGURE 3.12 Summary of the imaging process of a gamma camera. A count contributing to pixel *a* in the image is the result of the photomultiplier arithmetic indicating that a scintillation event was localized at the corresponding *x*,*y* coordinates in the crystal and that the pulse amplitude fell within the energy window selected. The scintillation, in turn, was the result of a gamma ray originating in the body somewhere in the shaded cone (width exaggerated) with a trajectory fully contained in that cone. Because its energy fell within the window around the photopeak, that photon suffered no (or minimal) scatter as it traveled between the tissue and the crystal.

Planar vs SPECT

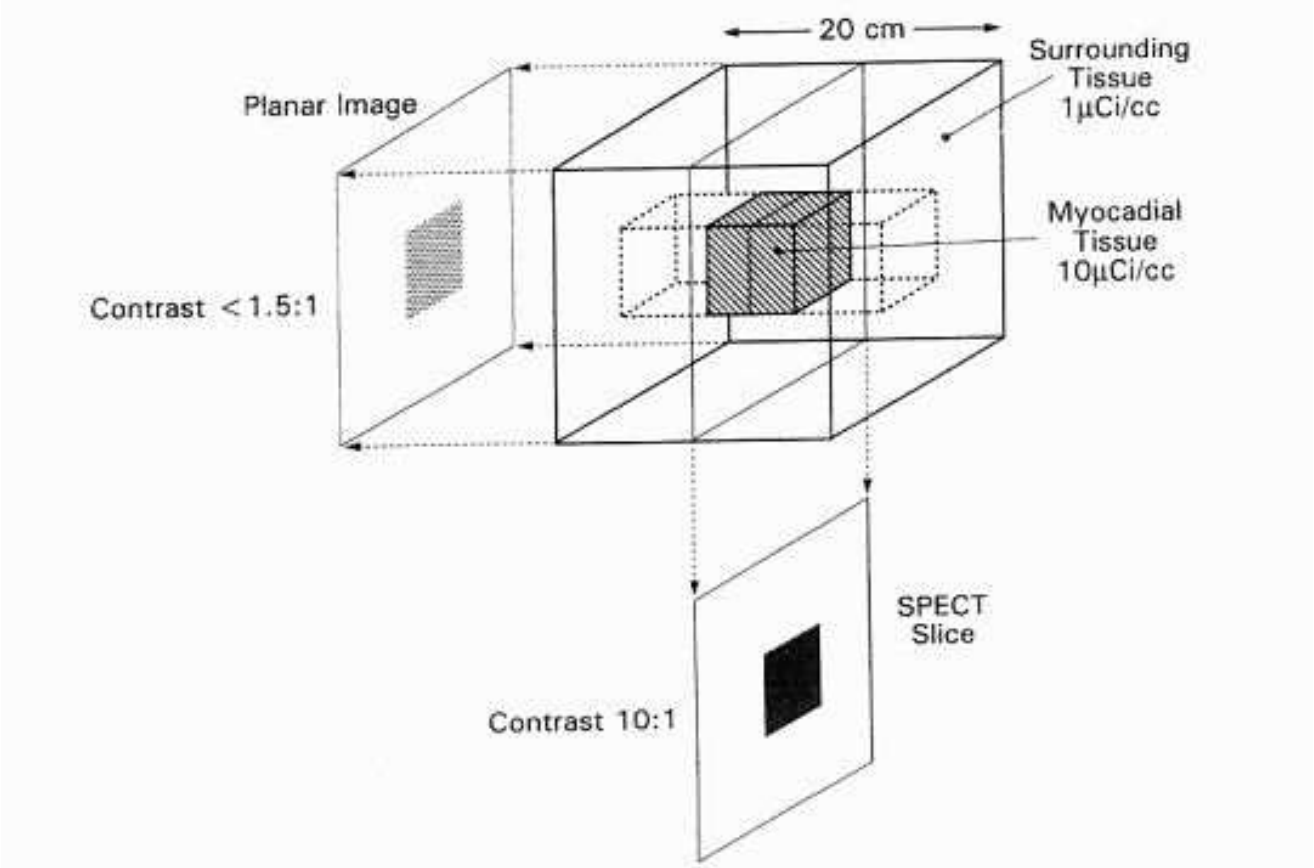

FIGURE 3.15 This model of tissue illustrates how tomography improves contrast. The planar image shown at the top left superimposes on the 'hot' area the background activity in front and behind (prism outlined with a dotted line) reducing the relative difference between hot and surrounding areas and therefore the contrast. In the tomographic slice shown below the hot area does not include background and thus the true, local difference in uptake is translated into actual image contrast. (For clarity, the small 1 cm per side cube representing the heart tissue is not drawn to scale.)

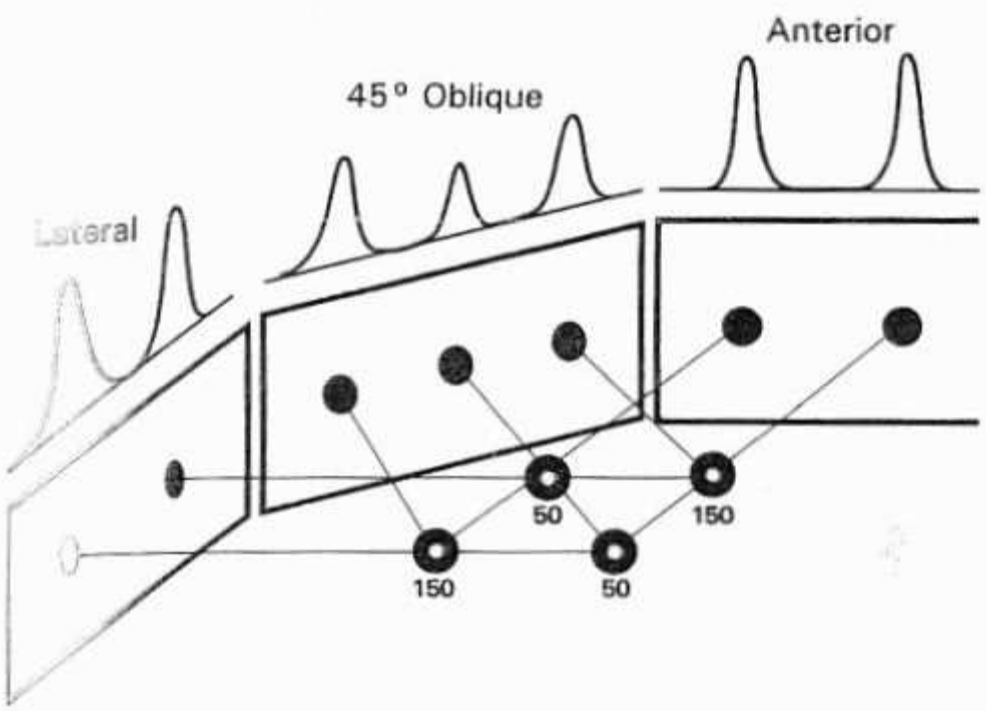

FIGURE 3.16 Rationale of tomographic reconstruction: individually, each of the three planar projections shown gives only an incomplete version of the real objects. The three projections together, while still not sufficient to reconstruct a view of the four objects, indicate that there are at least three objects and give a better idea of their activity. Additional projections will provide additional information necessary to reconstruct a slice view of the objects.

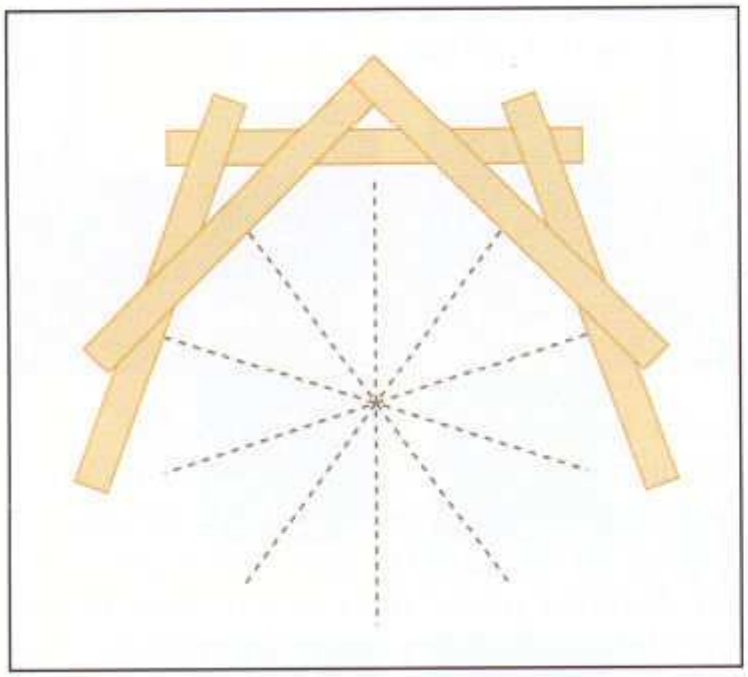

FIGURE 1-25. Backprojection of filtered data. The data from the ra
localized in three-dimensional space by backprojection of the filt
is localized along a line on the z axis from a single planar image.
z axes from the different planar images transect determines the l
along the z axis.

Reconstruction

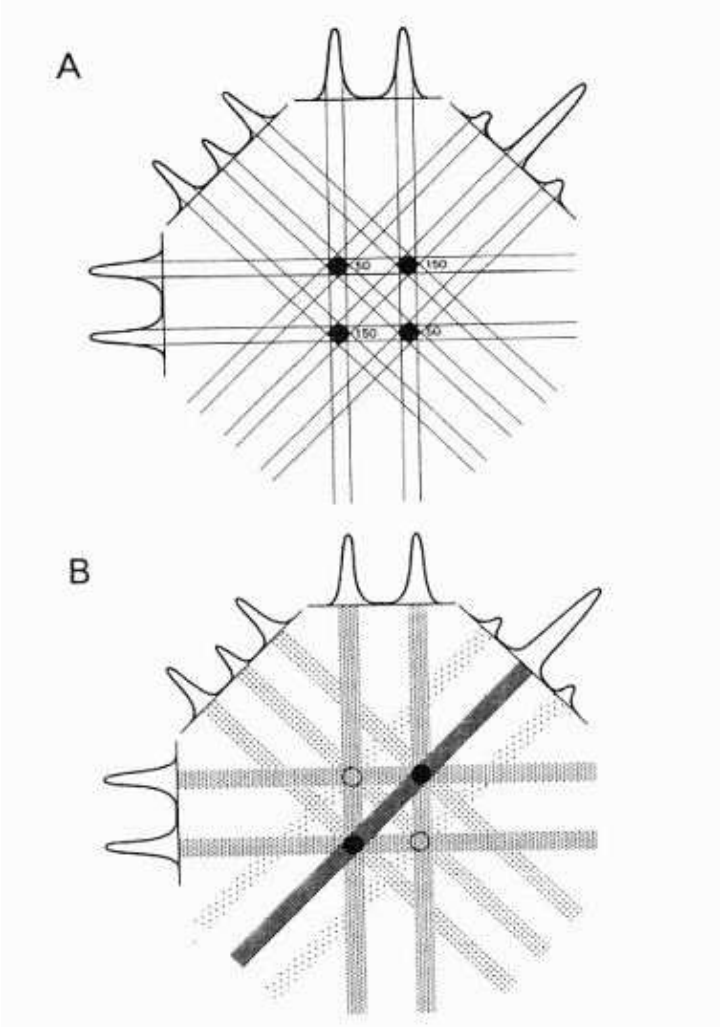

FIGURE 3.17 (*A*) Same "data" as in Figure 3.16 with an additional view showing only the count profiles. (*B*) The information in the count profiles (height and projection angle) is used to back-project beams of intensity proportional to the activity in the count profile onto a blank area. The superposition of these beams creates a tomographic view of the objects recorded by the projections. It also leaves a background of streaks to be removed by digitally filtering the image. The larger the number of projections the better the detail (in-plane resolution) and the more homogeneous the background of streaks.

Low and High Pass Filter

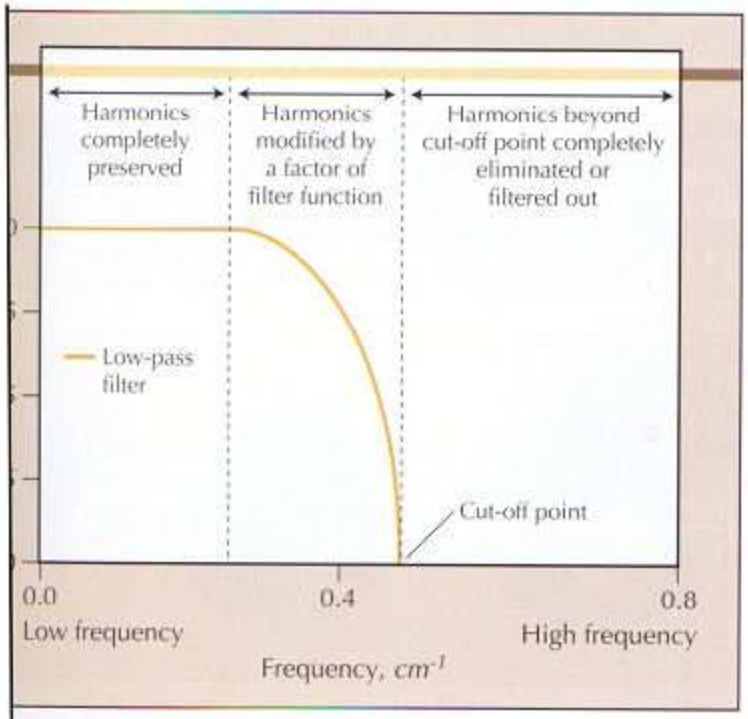

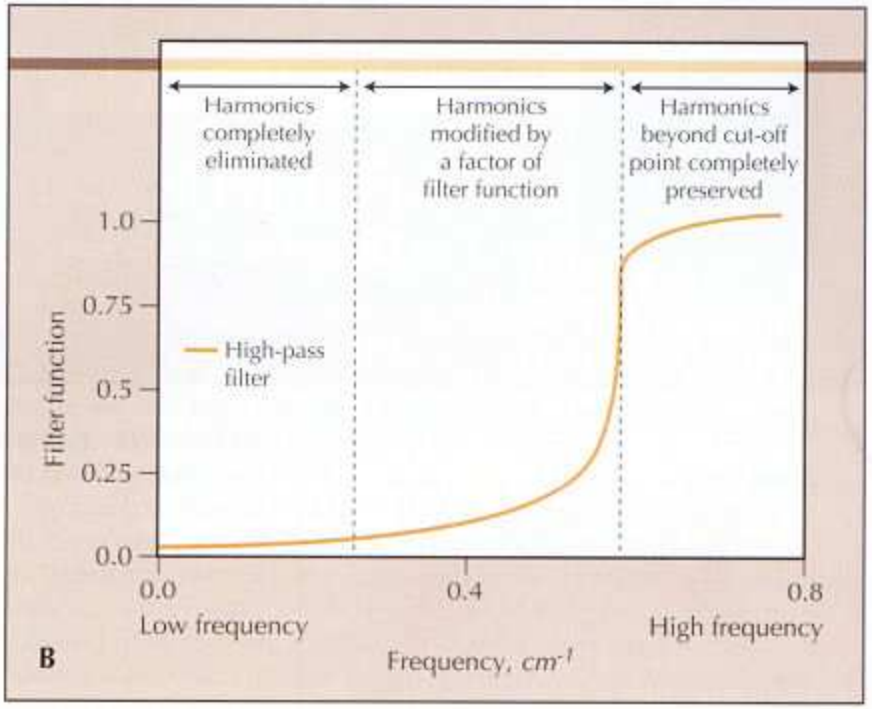

24. Filtering of SPECT images. The acquired raw images what noisy, and so filtering is required to eliminate or e noise. There are several ways of filtering out the noise. common way is by Fourier transformation of the raw which the image data are transformed into a series of es. The relevant data are present in the low-frequency ereas noise is present in the high-frequency range.

A, Low-pass filter allows the low frequencies to be retained unaltered and eliminates completely the high frequencies above the cut-off range. The frequencies in the intermediate range are altered by a function depicted by the slope of the cut-off curve. If too much filtering is used, even the useful data may be lost. **B**, The high-pass filter retains the high frequencies and eliminates the low frequencies. This filter is used primarily for edge enhancement.

Continued on next page

Filtered Raw

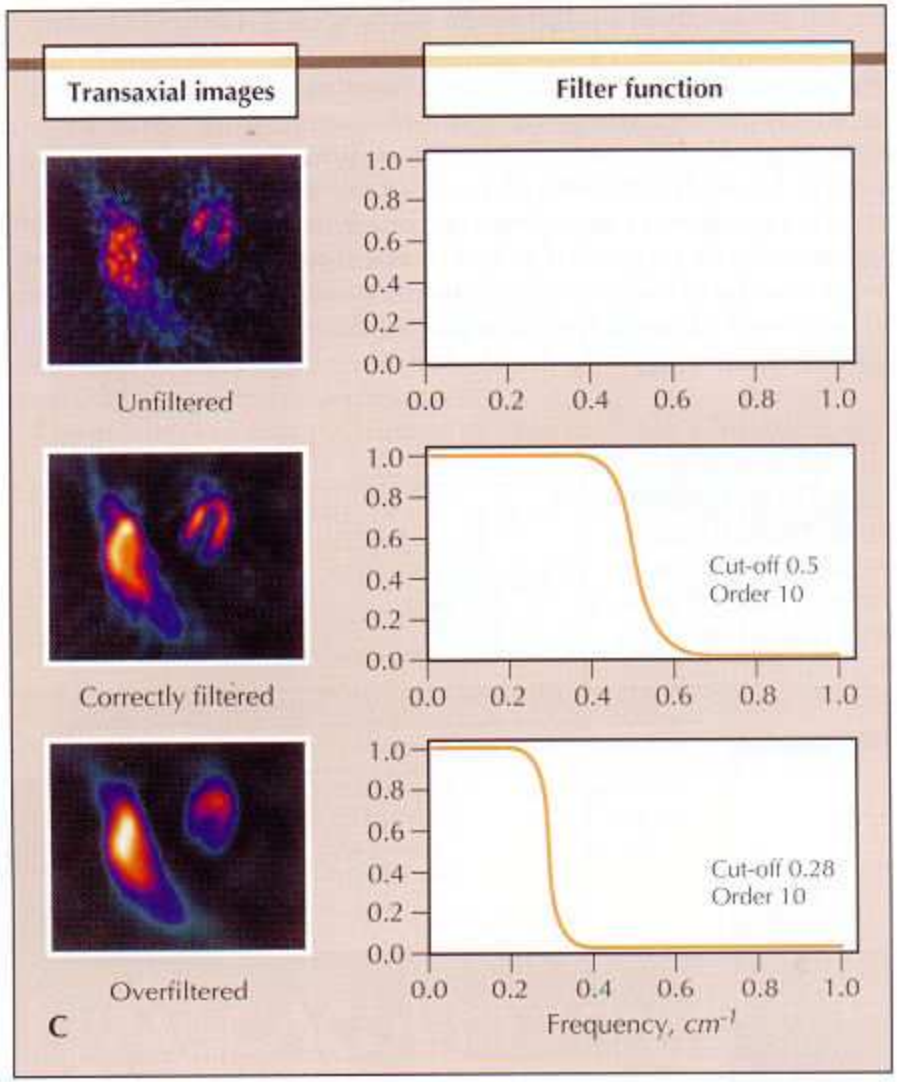

FIGURE 1-24. *(Continued)* **C,** A patient exampl
filter (Butterworth filter) is applied to transa
heart is shown. The unfiltered images *(top)*
very noisy. The background noise is elimina
filtered images *(center)*. However, overfilter
of the myocardial contour *(bottom)*.

Points about ^{201}Thallium

- Monovalent cation, biologic properties similar to potassium
- 80 keV mercury X-ray emission, 74 hour physical half life
- High first pass extraction(85%)
- Transported across myocyte sarcolemmal membrane by Na-K ATPase trasport AND facilitative diffusion
- Peak myocardial concentration within 5 minutes of IV injection
- Rapid intravascular clearance
- Redistribution begins 10-15 minutes after injection

Points about ^{99m}Tc

- Lipid soluble, cationic
- 140 keV photopeak energy, 6 hour physical half life
- First pass extraction 60%
- Uptake is passive across mitochondrial membranes
- At equilibrium, it is retained within mitochondria due to large negative transmembrane potential
- Clearance from intravascular compartment by hepatobiliary excretion
- Minimal redistribution compared to ^{201}Tl

On to the scans…

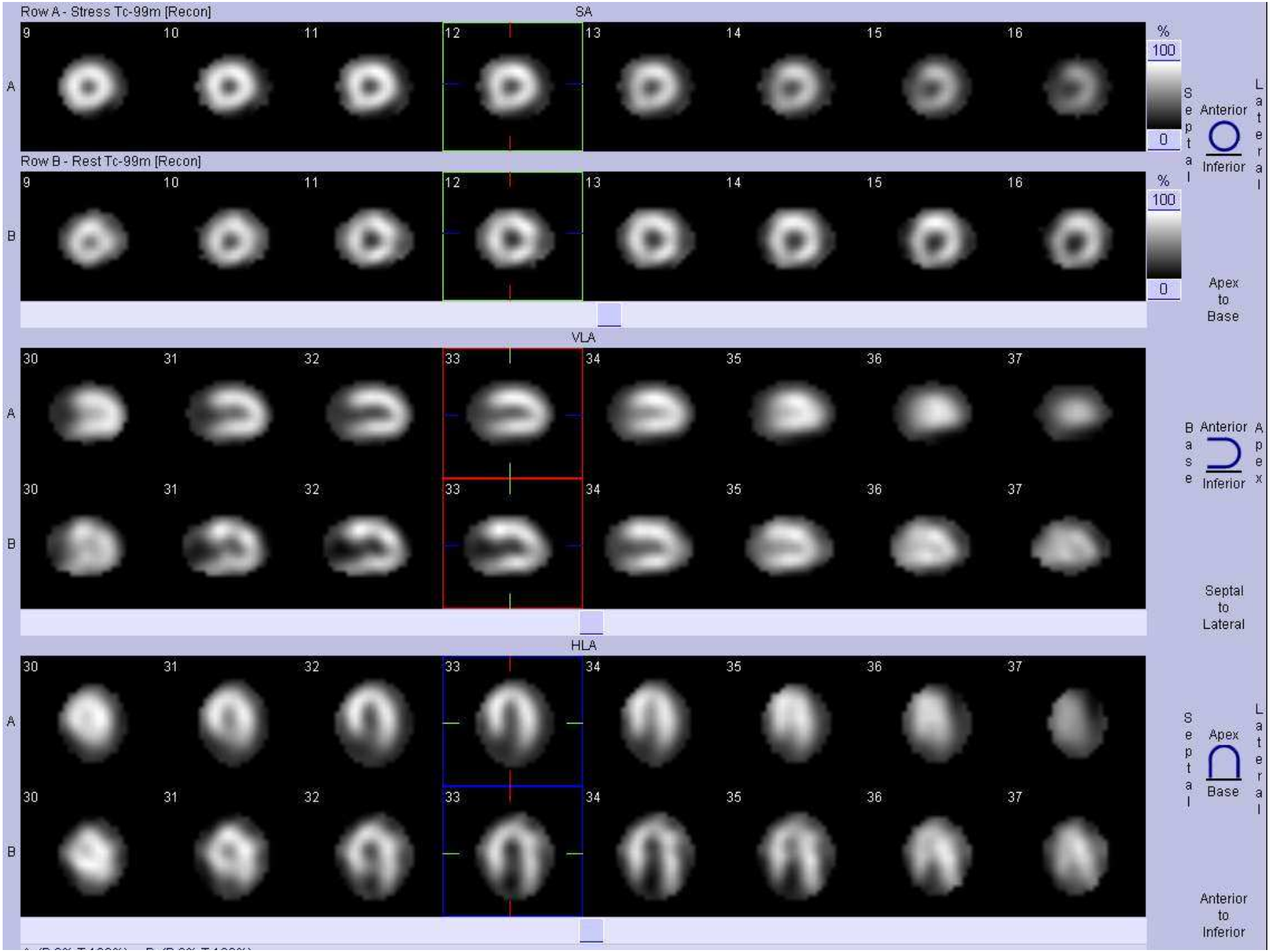
Row A - Stress Tc-99m [Recon]
SA
9 10 11 12 13 14 15 16
A
%
100
0
Septal
Anterior
Inferior
Lateral
Row B - Rest Tc-99m [Recon]
9 10 11 12 13 14 15 16
B
%
100
0
Apex to Base
VLA
30 31 32 33 34 35 36 37
A
Base
Anterior
Inferior
Apex
30 31 32 33 34 35 36 37
B
Septal to Lateral
HLA
30 31 32 33 34 35 36 37
A
Septal
Apex
Base
Lateral
30 31 32 33 34 35 36 37
B
Anterior to Inferior

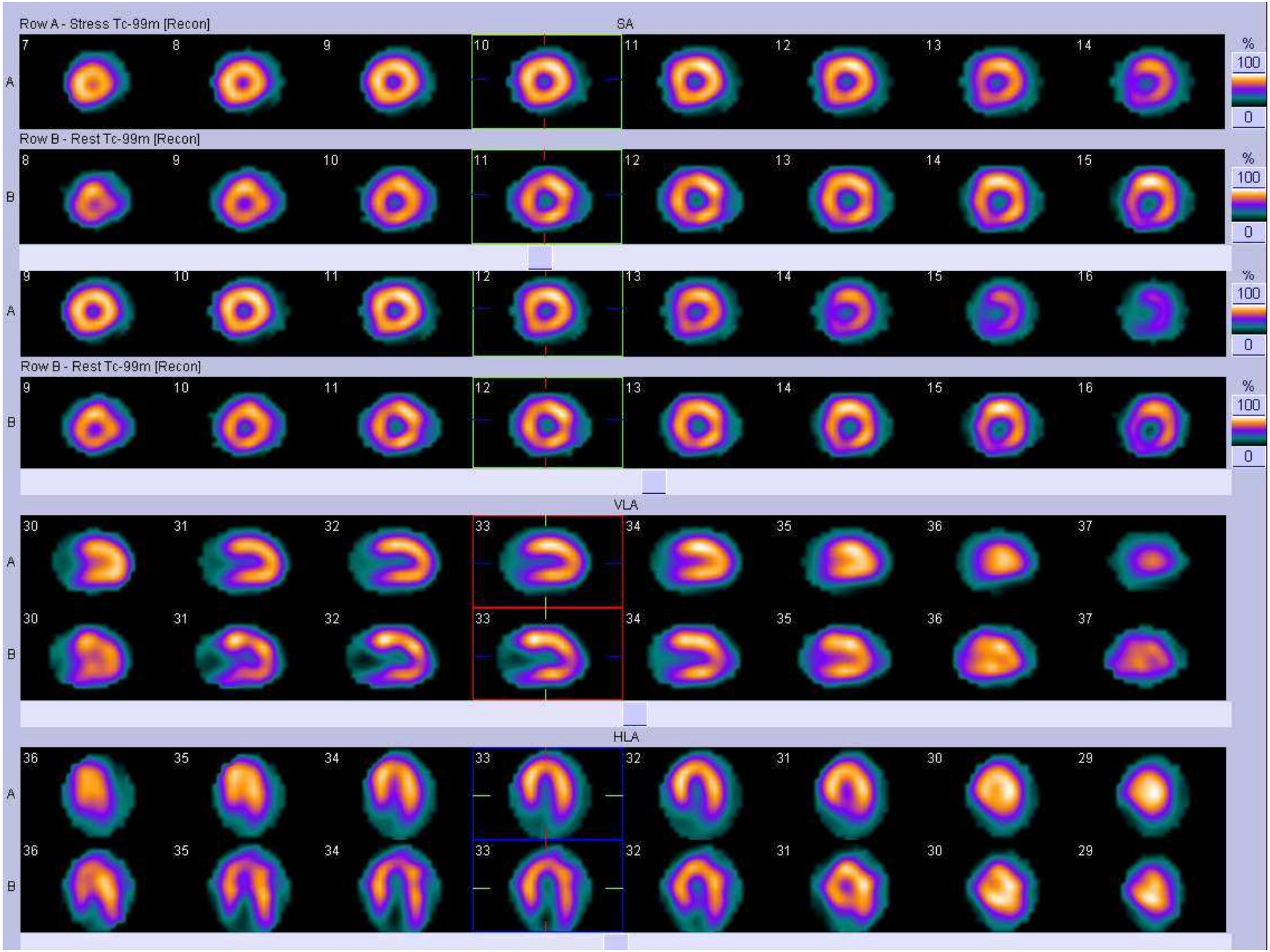
Row A - Stress Tc-99m [Recon]
SA
7 8 9 10 11 12 13 14
A
%
100
0
Row B - Rest Tc-99m [Recon]
8 9 10 11 12 13 14 15
B
%
100
0
9 10 11 12 13 14 15 16
A
%
100
0
Row B - Rest Tc-99m [Recon]
9 10 11 12 13 14 15 16
B
%
100
0
VLA
30 31 32 33 34 35 36 37
A
30 31 32 33 34 35 36 37
B
HLA
36 35 34 33 32 31 30 29
A
36 35 34 33 32 31 30 29
B

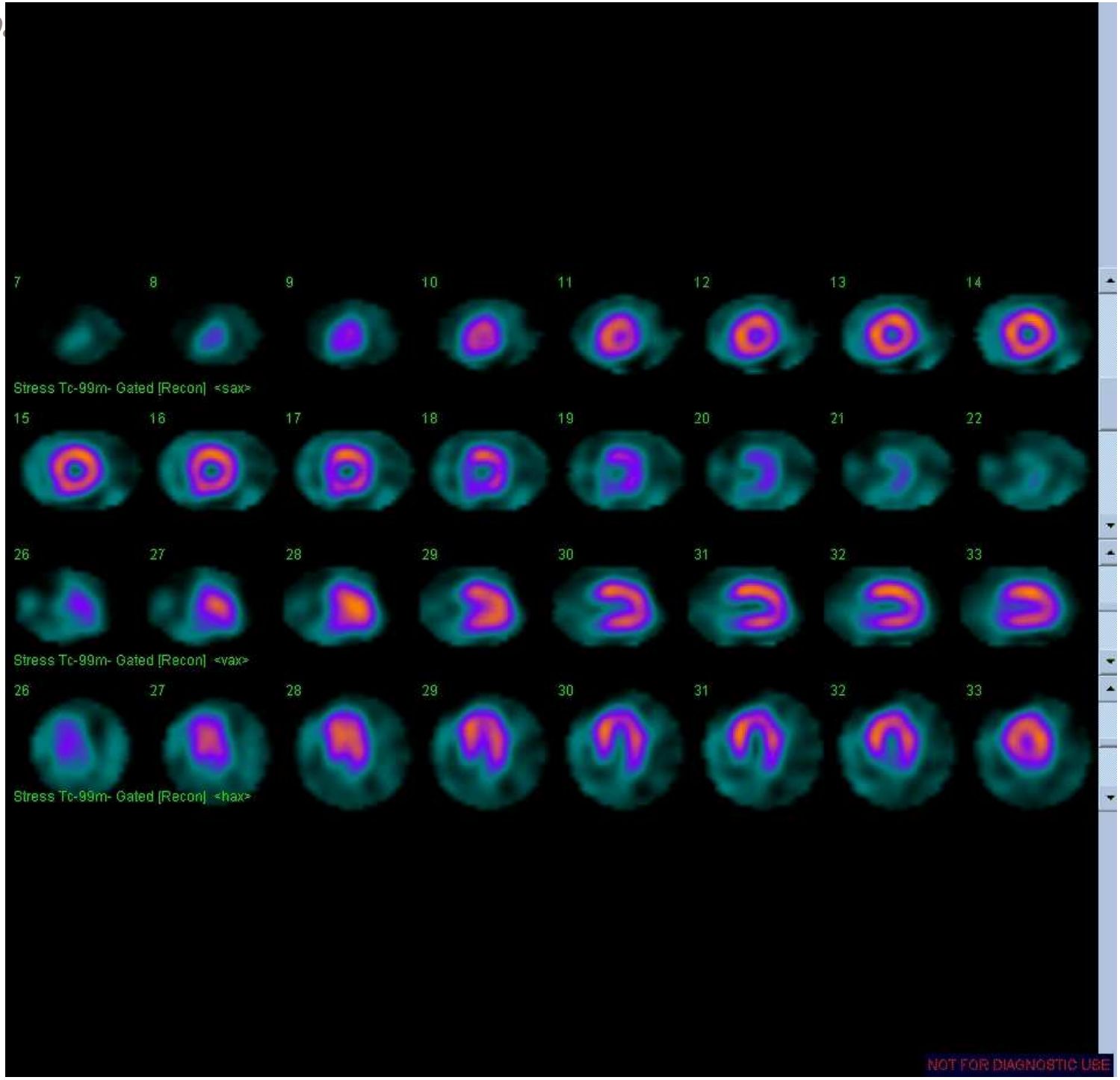
7 8 9 10 11 12 13 14
Stress Tc-99m- Gated [Recon] <sax>
15 16 17 18 19 20 21 22
26 27 28 29 30 31 32 33
Stress Tc-99m- Gated [Recon] <vax>
26 27 28 29 30 31 32 33
Stress Tc-99m- Gated [Recon] <hax>
NOT FOR DIAGNOSTIC USE

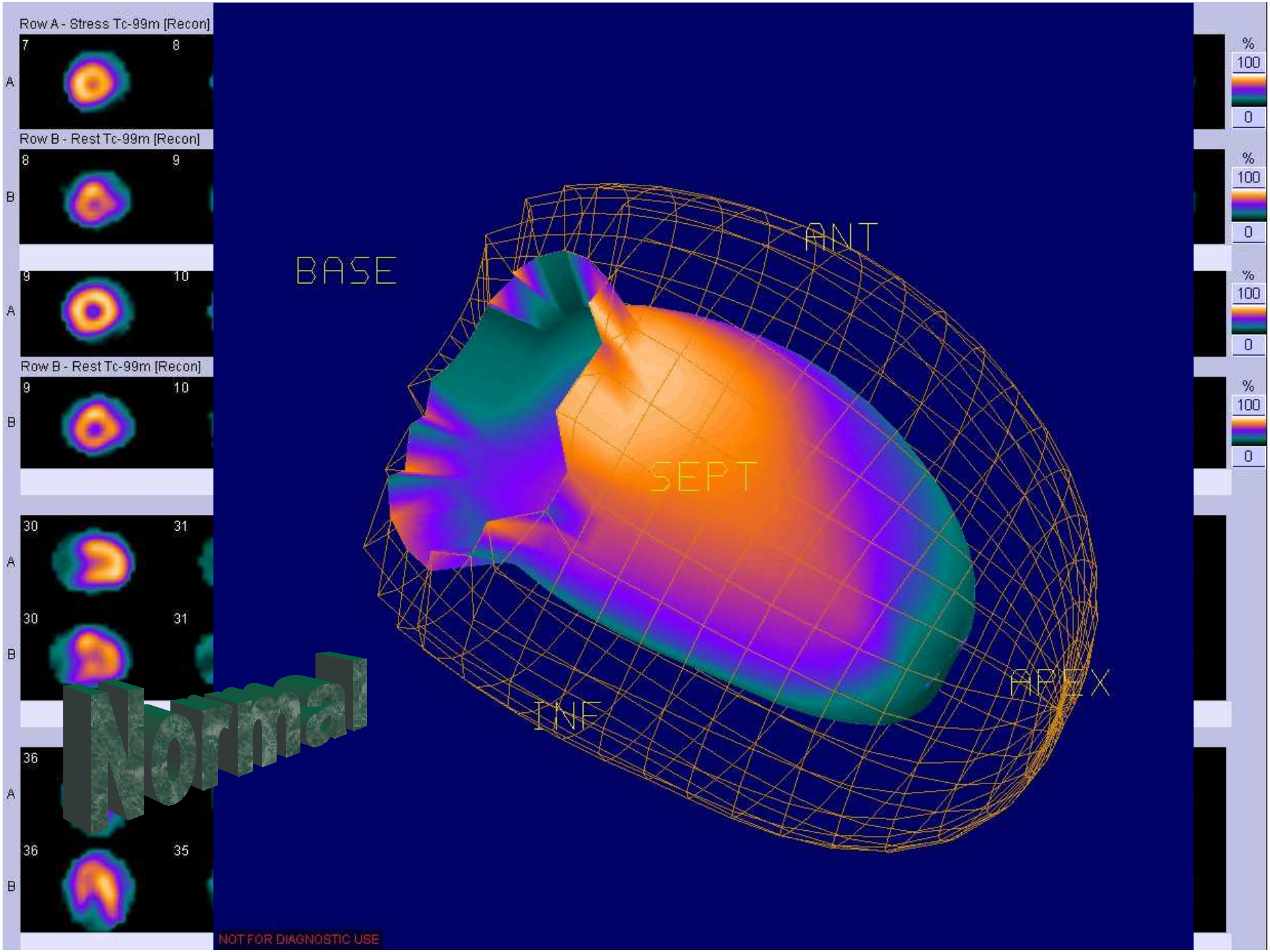
Row A - Stress Tc-99m [Recon]
7
8
A
Row B - Rest Tc-99m [Recon]
8
9
B
9
10
A
Row B - Rest Tc-99m [Recon]
9
10
B
30
31
A
30
31
B
36
A
36
35
B
BASE
ANT
SEPT
INF
APEX
Normal
%
100
0
%
100
0
%
100
0
%
100
0
NOT FOR DIAGNOSTIC USE

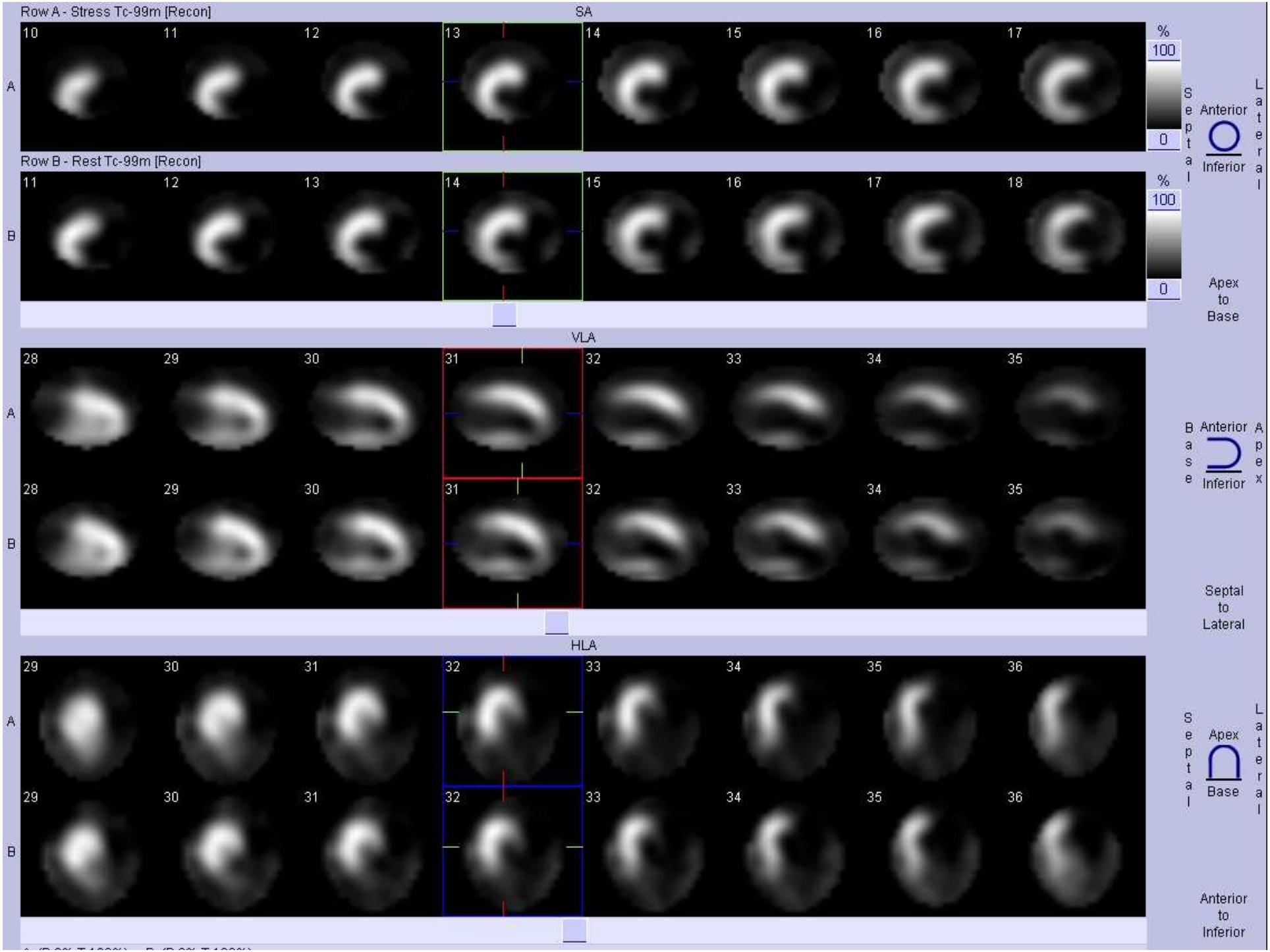
Row A - Stress Tc-99m [Recon]
SA
10 11 12 13 14 15 16 17
A
%
100
0
Septal
Anterior
Inferior
Lateral
Row B - Rest Tc-99m [Recon]
11 12 13 14 15 16 17 18
B
%
100
0
Apex to Base
VLA
28 29 30 31 32 33 34 35
A
Base
Anterior
Inferior
Apex
28 29 30 31 32 33 34 35
B
Septal to Lateral
HLA
29 30 31 32 33 34 35 36
A
Septal
Apex
Base
Lateral
29 30 31 32 33 34 35 36
B
Anterior to Inferior

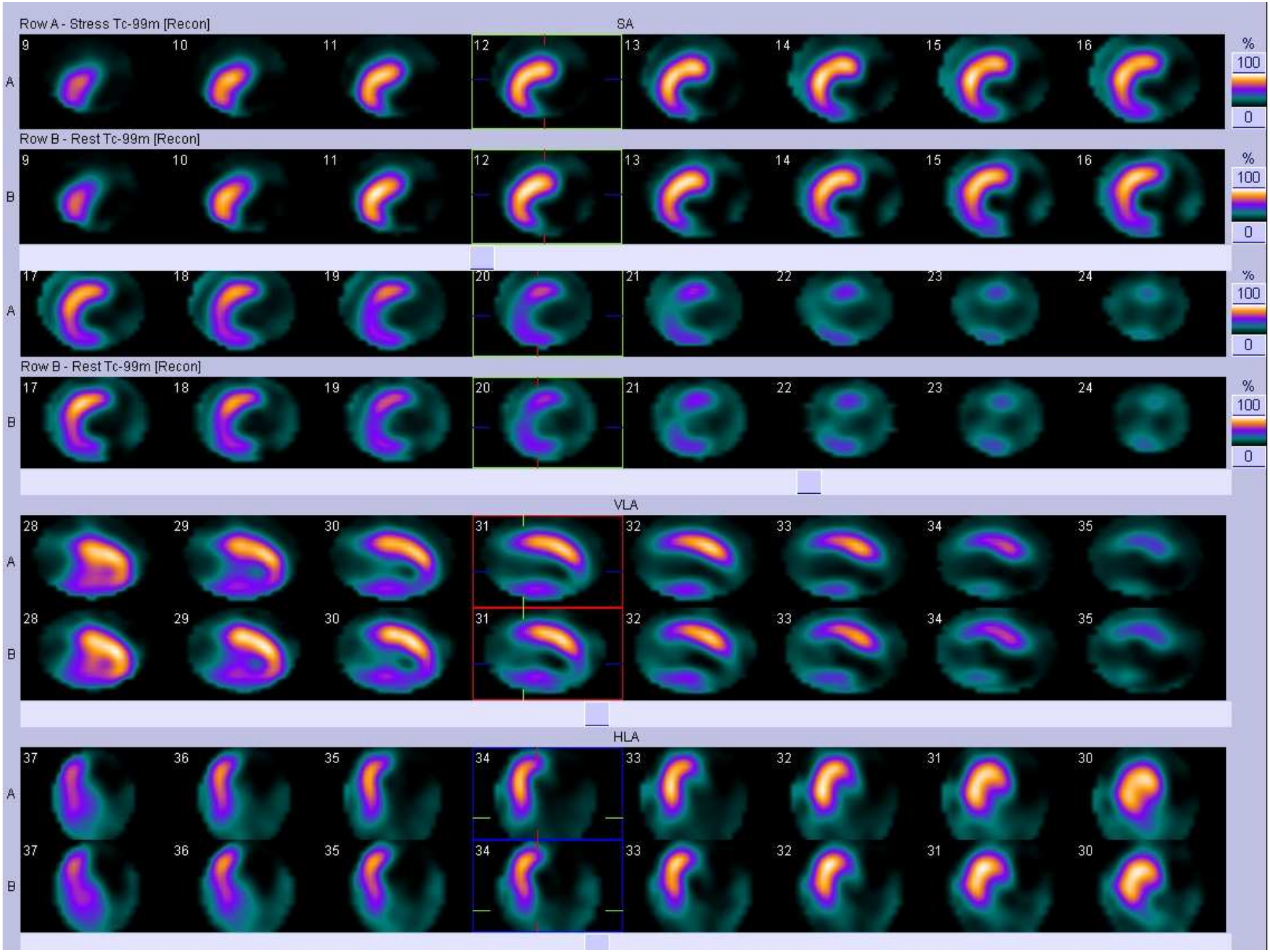
Row A - Stress Tc-99m [Recon]
SA
9
10
11
12
13
14
15
16
A
%
100
0
Row B - Rest Tc-99m [Recon]
9
10
11
12
13
14
15
16
B
%
100
0
17
18
19
20
21
22
23
24
A
%
100
0
Row B - Rest Tc-99m [Recon]
17
18
19
20
21
22
23
24
B
%
100
0
VLA
28
29
30
31
32
33
34
35
A
28
29
30
31
32
33
34
35
B
HLA
37
36
35
34
33
32
31
30
A
37
36
35
34
33
32
31
30
B

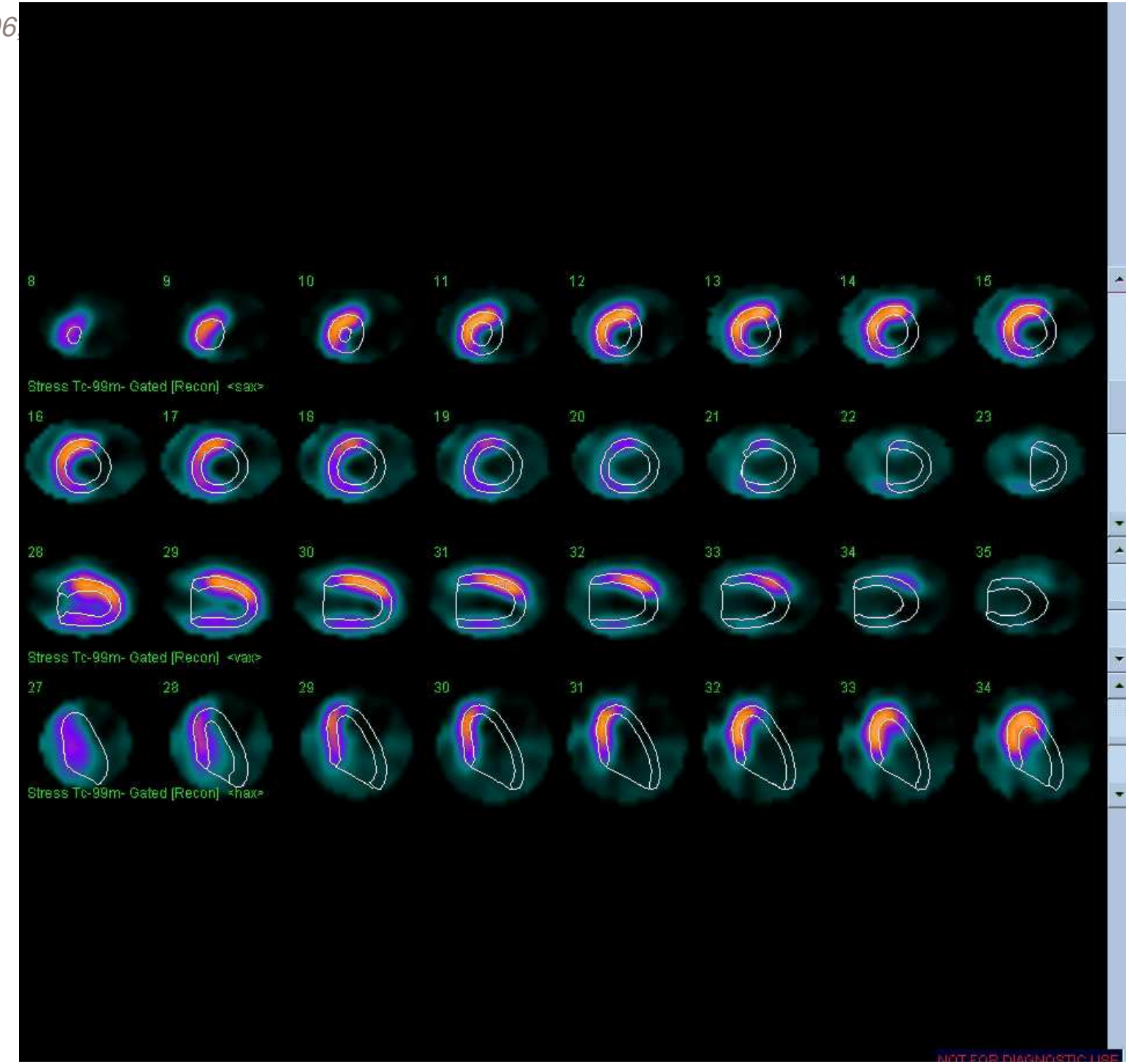
8
9
10
11
12
13
14
15
Stress Tc-99m- Gated [Recon] <sax>
16
17
18
19
20
21
22
23
28
29
30
31
32
33
34
35
Stress Tc-99m- Gated [Recon] <vax>
27
28
29
30
31
32
33
34
Stress Tc-99m- Gated [Recon] <hax>
NOT FOR DIAGNOSTIC USE

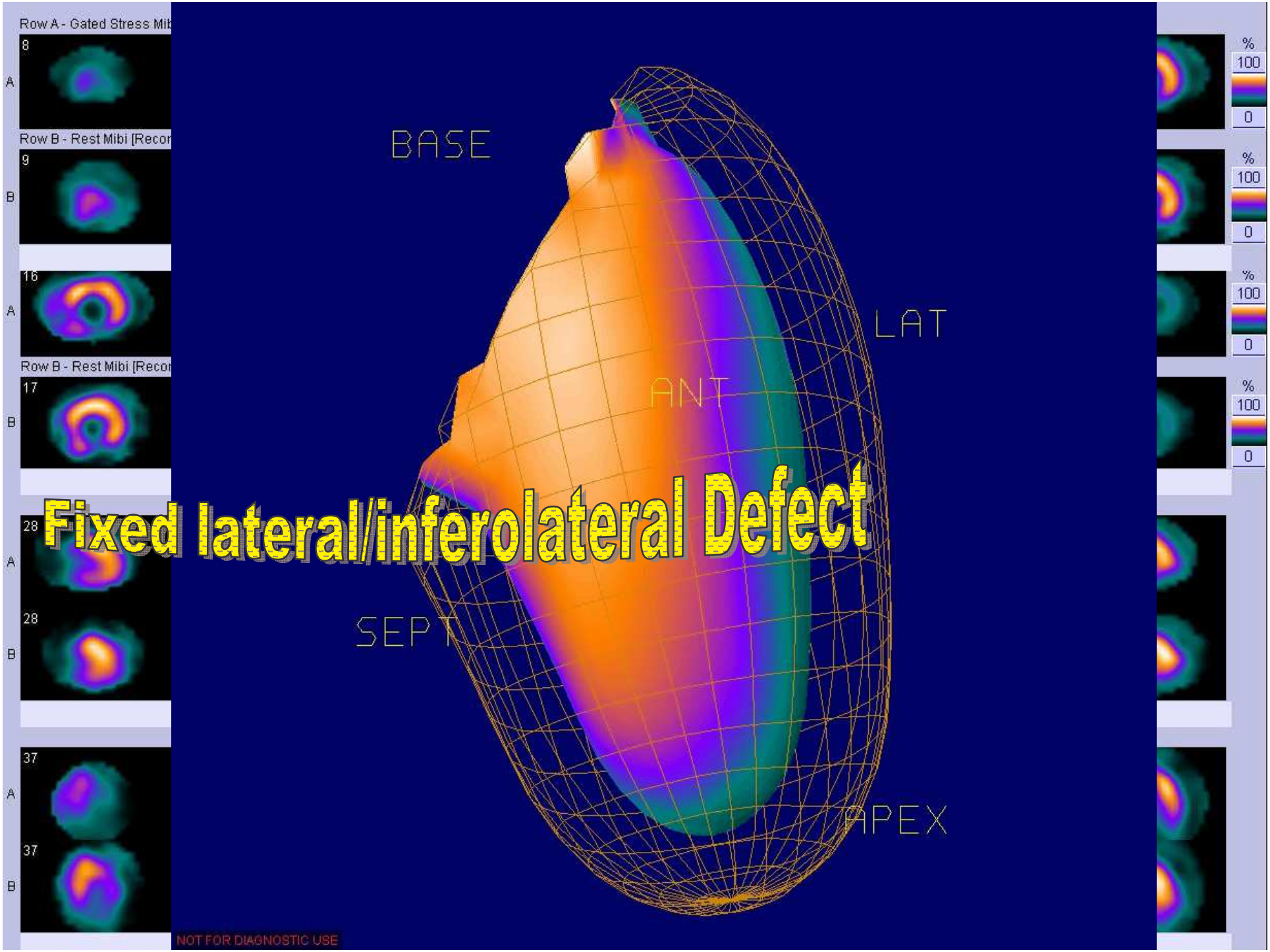
Row A - Gated Stress Mib
8
A
Row B - Rest Mibi [Recor
9
B
16
A
Row B - Rest Mibi [Recor
17
B
28
A
28
B
37
A
37
B
BASE
LAT
ANT
SEPT
APEX
%
100
0
Fixed lateral/inferolateral Defect
NOT FOR DIAGNOSTIC USE

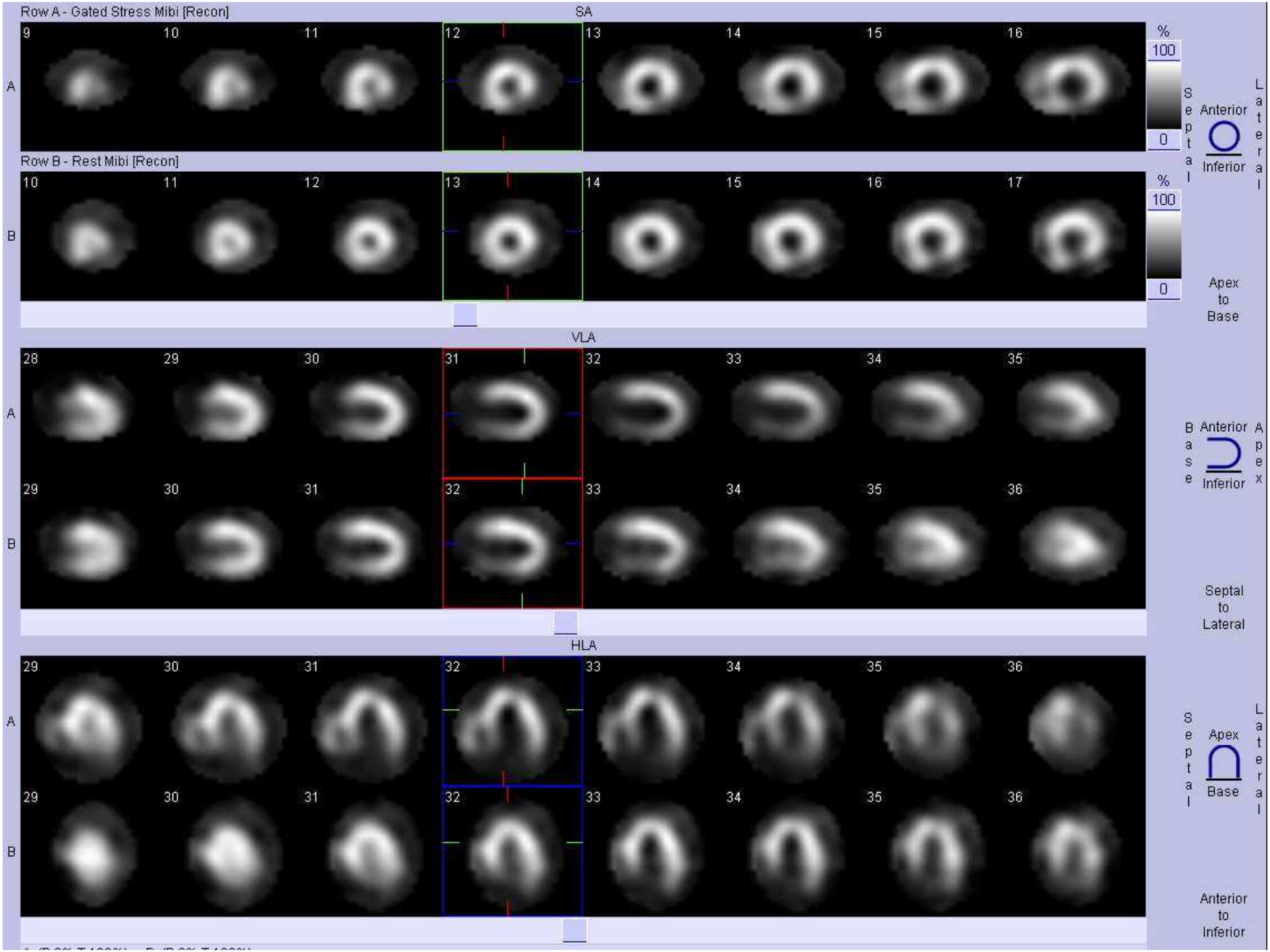
Row A - Gated Stress Mibi [Recon]
SA
9 10 11 12 13 14 15 16
%
100
0
Septal
Anterior
Inferior
Lateral
Row B - Rest Mibi [Recon]
10 11 12 13 14 15 16 17
%
100
0
Apex to Base
VLA
28 29 30 31 32 33 34 35
29 30 31 32 33 34 35 36
Base
Anterior
Inferior
Apex
Septal to Lateral
HLA
29 30 31 32 33 34 35 36
29 30 31 32 33 34 35 36
Septal
Apex
Base
Lateral
Anterior to Inferior

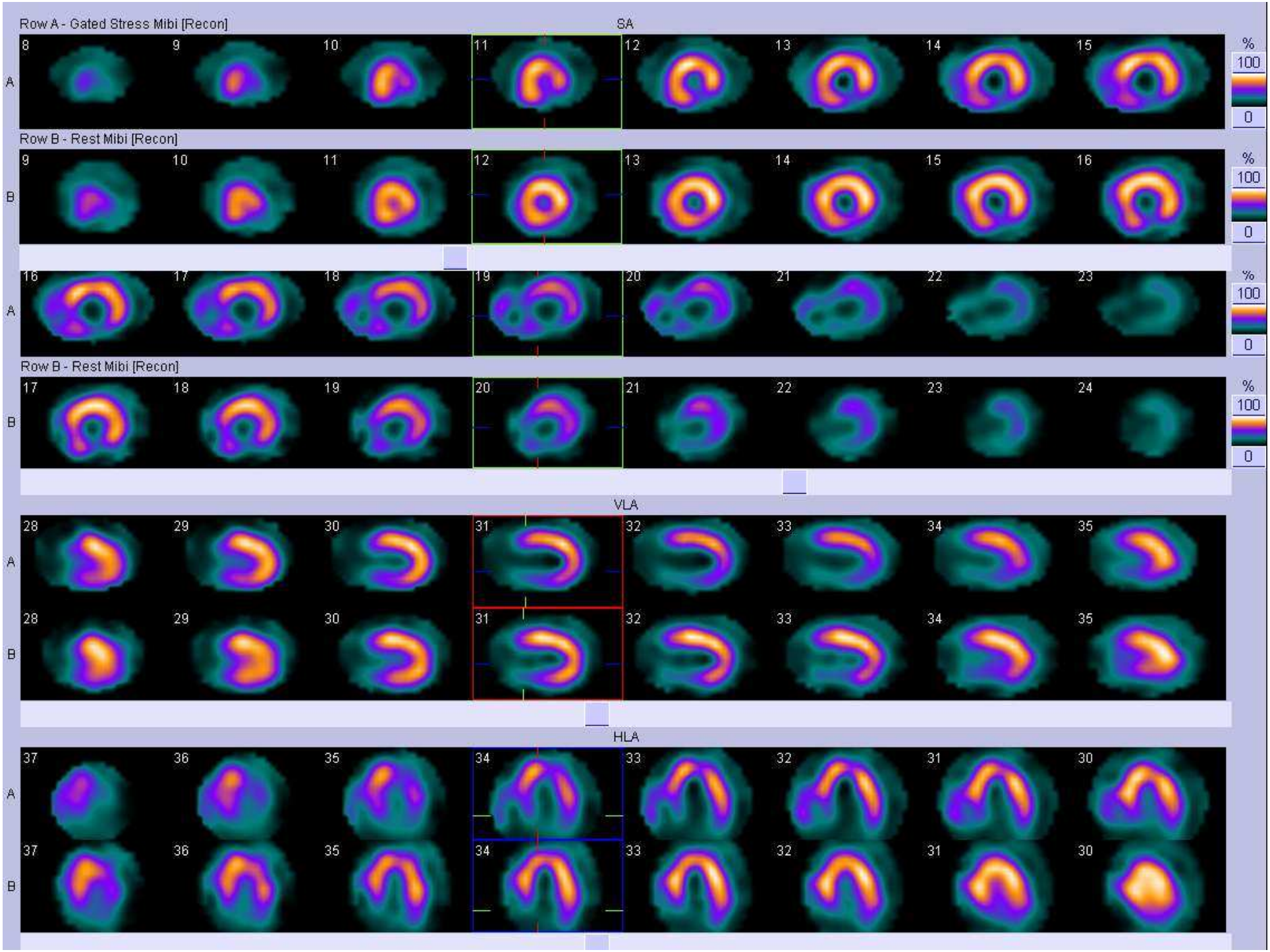
Row A - Gated Stress Mibi [Recon]
SA
8 9 10 11 12 13 14 15
A
%
100
0
Row B - Rest Mibi [Recon]
9 10 11 12 13 14 15 16
B
%
100
0
16 17 18 19 20 21 22 23
A
%
100
0
Row B - Rest Mibi [Recon]
17 18 19 20 21 22 23 24
B
%
100
0
VLA
28 29 30 31 32 33 34 35
A
28 29 30 31 32 33 34 35
B
HLA
37 36 35 34 33 32 31 30
A
37 36 35 34 33 32 31 30
B

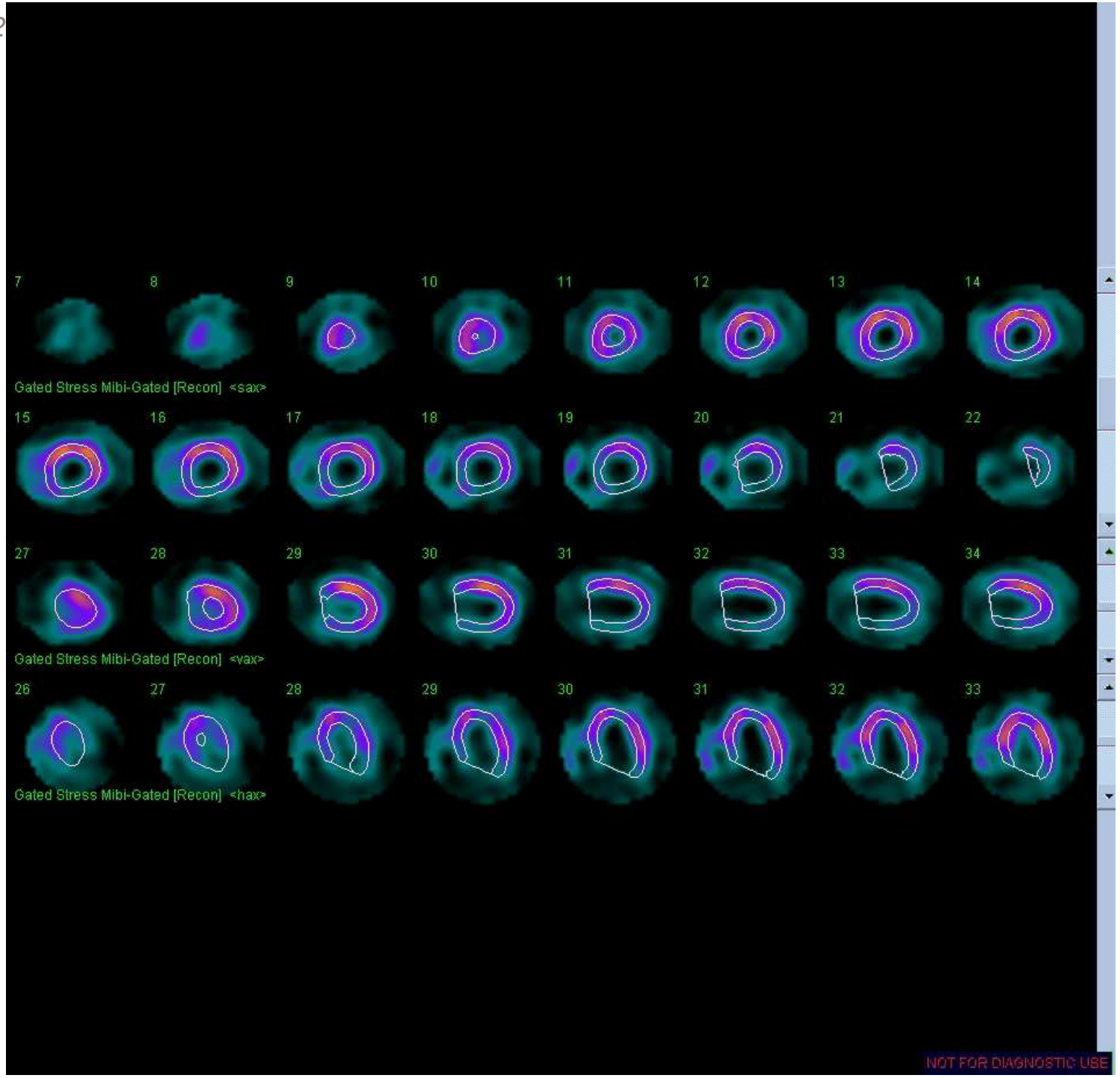
7
8
9
10
11
12
13
14
Gated Stress Mibi-Gated [Recon] <sax>
15
16
17
18
19
20
21
22
27
28
29
30
31
32
33
34
Gated Stress Mibi-Gated [Recon] <vax>
26
27
28
29
30
31
32
33
Gated Stress Mibi-Gated [Recon] <hax>
NOT FOR DIAGNOSTIC USE

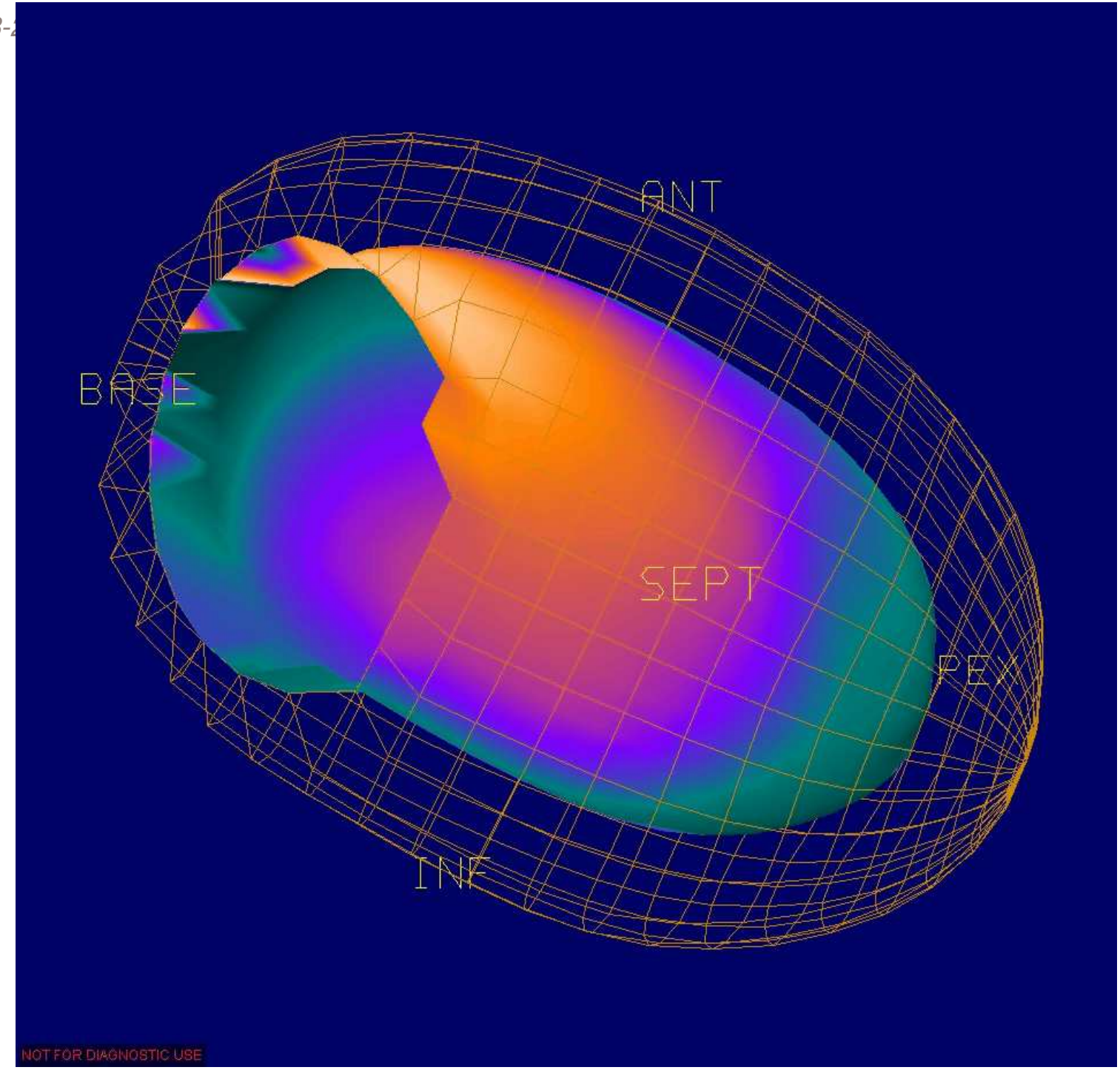

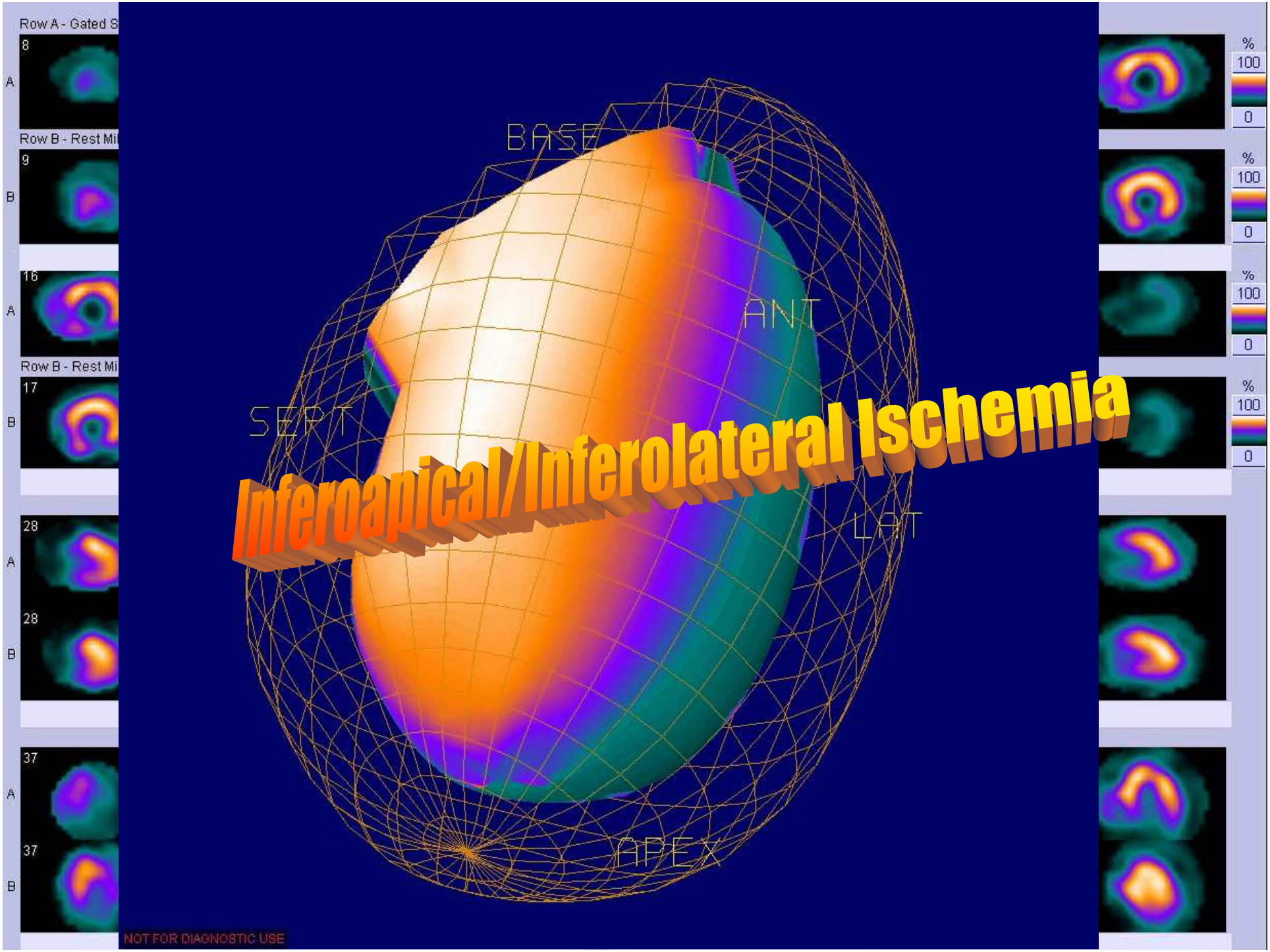
Row A - Gated S
8
A
Row B - Rest Mi
9
B
16
A
Row B - Rest Mi
17
B
28
A
28
B
37
A
37
B
BASE
ANT
SEPT
LAT
APEX
Inferoapical/Inferolateral Ischemia
%
100
0
NOT FOR DIAGNOSTIC USE

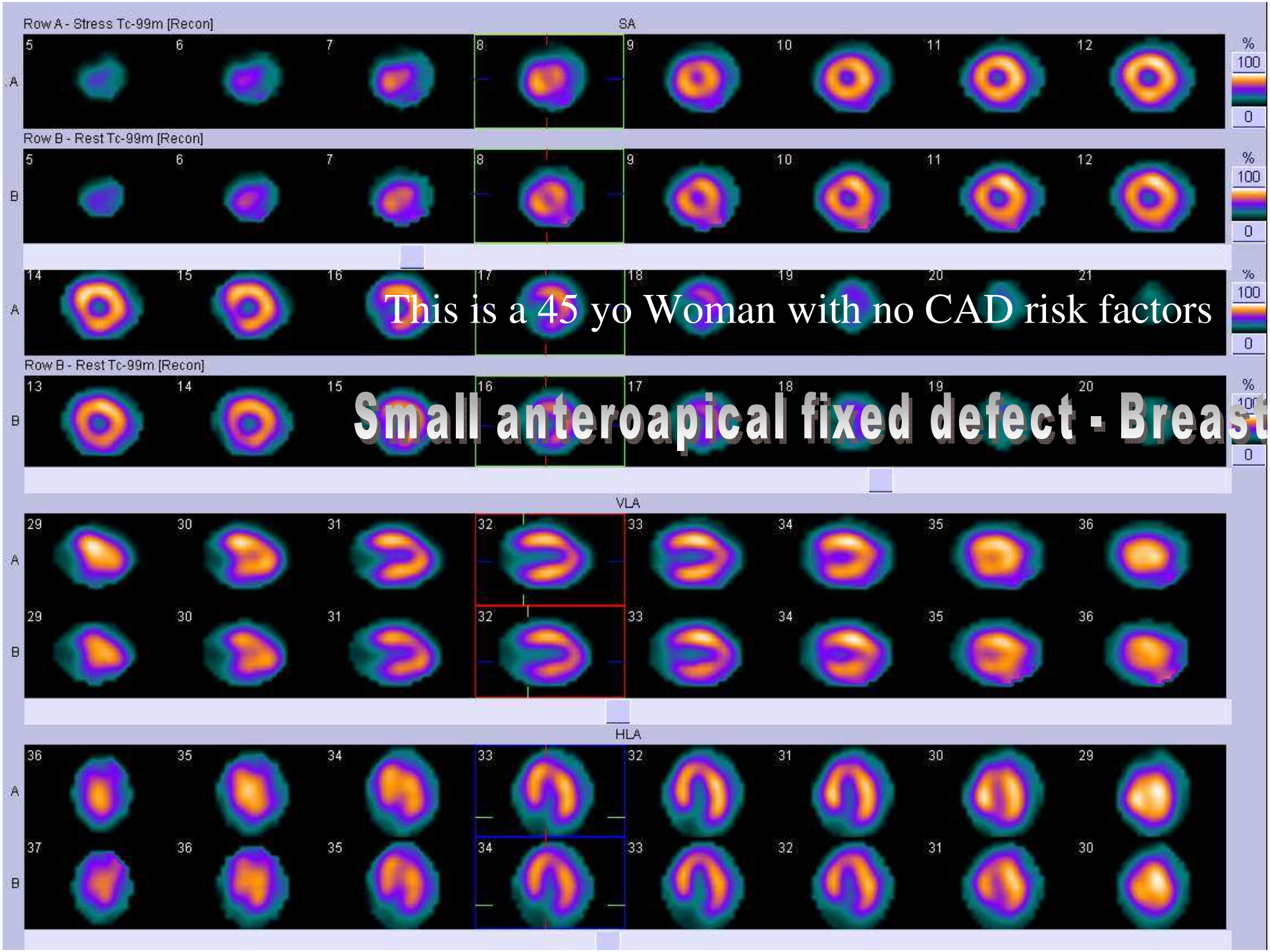
Row A - Stress Tc-99m [Recon]
SA
Row B - Rest Tc-99m [Recon]
Row B - Rest Tc-99m [Recon]
VLA
HLA
This is a 45 yo Woman with no CAD risk factors
Small anteroapical fixed defect - Breast